R77-912506-14

CR-135196

Graphite Fiber Reinforced Thermoplastic Resins

By

R.C. Novak

United Technologies Research Center

East Hartford, Ct. 06108

Prepared for

National Aeronautics and Space Administration

NASA Lewis Research Center

Contract NAS3-20077

Kenneth Bowles, Project manager

1. Report No.	2. Government Accession No.	3. Recipient's Catalog No.
NASA CR-135196		

4. Title and Subtitle	5. Report Date
GRAPHITE FIBER REINFORCED THERMOPLASTIC RESINS	April 18, 1977
	6. Performing Organization Code

7. Author(s)	8. Performing Organization Report No.
Richard C. Novak	R77-912506-14
	10. Work Unit No.

9. Performing Organization Name and Address	11. Contract or Grant No.
United Technologies Research Center East Hartford, CT 06108	NAS3-20077
	13. Type of Report and Period Covered
12. Sponsoring Agency Name and Address	Contractor Report - Final
National Aeronautics and Space Agency Structures Division, NASA-Lewis Research Center Cleveland, OH 44135	14. Sponsoring Agency Code

15. Supplementary Notes

Project Manager, Kenneth Bowles, Materials & Structures Division, NASA Lewis Research Center, Cleveland, OH 44135

16. Abstract

This report describes the results of a program designed to optimize the fabrication procedures for graphite/thermoplastic composites, measure the properties of the composites as a function of temperature and finally, to fabricate and test graphite/thermoplastic fan exit guide vanes. Three thermoplastics were included in the investigation: polysulfone, polyethersulfone, and polyarylsulfone. Type HMS graphite was used as the reinforcement.

It was found that good quality composites having good mechanical properties could be fabricated with polysulfone and polyethersulfone matrix composites, but successful processing of polyarylsulfone composites was not achieved. Based on static shear, flexural, and tensile properties and tensile stress-rupture testing the upper use temperature of polysulfone matrix composites is somewhat less than 149°C, for polyethersulfone matrix composites it is under 177°C, while the polyarylsulfone composites showed little effect of temperature at 232°C.

Bending fatigue tests of HMS graphite/polyethersulfone demonstrated a gradual shear failure mode which resulted in a loss of stiffness in the specimens. Preliminary curves were generated to show the loss in stiffness as a function of stress and number of cycles.

Fan exit guide vanes of HMS graphite/polyethersulfone were satisfactorily fabricated in the final phase of the program. These were found to have higher stiffness and better fatigue behavior than graphite/epoxy vanes which were formerly bill-of-material.

17. Key Words (Suggested by Author(s))	18. Distribution Statement
Laminating Resins Graphite Composites Thermoplastics Fabrication Mechanical Properties	Unclassified - Unlimited

19. Security Classif. (of this report)	20. Security Classif. (of this page)	21. No. of Pages	22. Price*
Unclassified	Unclassified		

* For sale by the National Technical Information Service, Springfield, Virginia 22161

Graphite Fiber Reinforced Thermoplastic Resins

TABLE OF CONTENTS

TABLE OF CONTENTS (Cont'd)

LIST OF TABLES

LIST OF ILLUSTRATIONS

SUMMARY

This report describes the results of a program designed to optimize the fabrication procedures for graphite/thermoplastic composites, measure the properties of the composites as a function of temperature and finally, to fabricate and test graphite/thermoplastic fan exit guide vanes. Three thermoplastics were included in the investigation: polysulfone, polyethersulfone, and polyarylsulfone. Type HMS graphite was used as the reinforcement.

It was found that good quality composites having good mechanical properties could be fabricated with polysulfone and polyethersulfone matrix composites, but successful processing of polyarylsulfone composites was not achieved. Based on static shear, flexural, and tensile properties and tensile stress-rupture testing the upper use temperature of polysulfone matrix composites is somewhat less than 149°C, for polyethersulfone matrix composites it is under 177°C, while the polyarylsulfone composites showed little effect of temperature at 232°C.

Bending fatigue tests of HMS graphite/polyethersulfone demonstrated a gradual shear failure mode which resulted in a loss of stiffness in the specimens. Preliminary curves were generated to show the loss in stiffness as a function of stress and number of cycles.

Fan exit guide vanes of HMS graphite/polyethersulfone were satisfactorily fabricated in the final phase of the program. These were found to have higher stiffness and better fatigue behavior than graphite/epoxy vanes which were formerly bill-of-material.

1.0 INTRODUCTION

This program follows Contract NAS3-17833, "Graphite Fiber Reinforced Thermoplastic Resins" (Ref. 1) which United Technologies Research Center undertook in order to characterize the mechanical behavior of thermoplastic resins in neat and reinforced form. The earlier program placed emphasis on determining the effects of various environmental exposures on the mechanical properties of the composites. In addition, two complex hardware items, a third stage fan blade and a fan exit guide vane, were fabricated from graphite/thermoplastic in order to study the feasibility of producing gas turbine engine structural components.

The primary conclusion of the study was that the two thermoplastics investigated, P-1700 polysulfone and Astrel 360 polyarylsulfone, were generally as good or better than a baseline epoxy (PR-286) in resisting the various environmental exposures. The P-1700 polysulfone was selected for the fabrication study and both articles were fabricated without difficulty.

Although the results were generally positive, areas warranting further study were identified. Properties had a rather wide scatter band in some cases, indicating the need for further optimization of the impregnation/fabrication process. Of the two thermoplastics, Astrel 360 polyarylsulfone had higher temperature capability than required for the engine applications of interest, while P-1700 polysulfone appeared to have a marginal upper use temperature. A material with an intermediate use temperature would be more desirable. Finally, the utility of the materials in engine applications could be substantiated only through a test program in which structures were subjected to conditions representative of those in an engine environment.

The current program, conducted by United Technologies Research Center with the Commercial Products Division of Pratt & Whitney Aircraft Group as a subcontractor, was directed toward expanding the technology in the areas indicated by the first contract.

The objectives of this program were to optimize the quality of graphite-thermoplastic composites through investigation of processing conditions and to evaluate the performance of the optimized materials in both specimen and hardware testing.

The program was divided into three technical tasks. During Task I the conditions for processing of three thermoplastic resin composites were optimized insofar as their effect on flexural and shear properties. Resins studied included polysulfone, polyethersulfone, and polyarylsulfone. The reinforcement for all composites was HMS graphite. Both prepreg preparation and composite consolidation parameters were studied.

Under Task II the optimized techniques were used to fabricate composites of each system and the following properties were measured:

1) tensile strength ($\pm$45°)
2) flexural strength (0°)
3) interlaminar shear strength (0°)
4) impact strength (0°)
5) creep/stress rupture ($\pm$45°)

Following that testing one material system was selected for fatigue testing, and one resin was used to evaluate the effect of a hybrid graphite/glass reinforcement.

In Task III the selected material was used to fabricate fan exit guide vanes of the type used in large gas turbine engines. These vanes were tested for stiffness, natural frequency, and fatigue performance. Prepreg of the selected material was prepared by United Technologies Research Center, and the vane fabrication and testing was conducted by the Commercial Products Division of Pratt & Whitney Aircraft Group.

The experimental procedures employed during this program and the results derived from it are discussed in the following sections.

2.0 TASK I - IMPROVED MATERIALS PROCESSING

The primary objective of this task was to determine the optimum processing techniques for unidirectional graphite reinforced composites having three different thermoplastic resins as matrix. In addition the applicability of the selected processing technique to a hybrid composite was to be determined for one of the resins. Primary evaluation criteria were void contents as determined by microscopic observation, and mechanical properties of the unidirectional composites.

2.1 Experimental Procedure

2.1.1 Test Plan

Both impregnation techniques and composite consolidation cycles were evaluated for each of the matrix materials. Impregnation variables included solvent, solution concentration, use of wetting agent, winding speed, winding tension, and drying conditions. Consolidation parameters were time, temperature, and pressure involved in the molding cycle.

A unidirectional composite was made from the impregnated tape resulting from each processing trial. A sample from the composite was metallographically prepared and examined under the light microscope, primarily to observe fiber distribution and void content. Those specimens which appeared to be of good quality were then tested to measure short beam shear and flexural properties. Final selection of processing conditions was based on a combination of good fiber distribution, low void content, and high mechanical properties.

2.1.2 Materials

The three thermoplastics evaluated were P-1700 polysulfone, Astrel 360 polyarylsulfone, and 300P polyethersulfone. The P-1700 and 300P were in pellet form, while the Astrel 360 was in a powdery form having a wide range of particle sizes. In order to make the powder more uniform it was passed through a screen and only the -200 mesh material was used.

The graphite fiber was HMS in a 10,000 filament tow with no sizing.

2.1.3 Fabrication

All materials were impregnated by passing the fiber through a solvent resin solution and winding on a take-up drum to form a unidirectional prepreg tape. The specific details of this process were varied during the course of this task

as described in Section 2.2. Following the winding, the tape was cut from the drum and dried to remove solvent. Composite consolidation was carried out between electrically-heated platens of a hydraulic press using steel molds to produce specimens nominally 3.75 cm x 15 cm x .25 cm (1 1/2 in. x 6 in. x .1 in.).

2.1.4 Test Techniques

Short beam shear specimens were .63 cm (.25 in.) wide and were tested in three point bending at a span-to-depth ratio of 4:1. Flexural specimens were the same width but were tested at a span-to-depth ratio of 32:1. In both cases the crosshead speed was 0.125 cm/min (0.05 in./min).

2.2 Results and Discussion

2.2.1 Polysulfone Matrix Composites

The fabrication trials which were conducted with P-1700 polysulfone matrix composites are listed in Table I. Nearly all runs were made with HMS fiber with the P-1700 polysulfone concentration varying from 7.5 to 11% in a solvent of pure methylene chloride or a mixture of equal parts methylene chloride and trichloroethylene. The winding conditions include the speed of yarn travel, and the number of pulleys the yarn passed under in the impregnation bath. The method used to remove solvent from the tape and the hot pressing conditions are given and the notes primarily indicate those instances in which a wetting agent, Tergitol NP-14, was added to the impregnation bath.

The primary objective of these trials was to achieve better impregnation of the center of the graphite bundles. Resin concentration was lowered in order to reduce solution viscosity. Trichloroethylene was added to the solvent to slow evaporation rates and to encourage better penetration by better wetting. The winding speed and the number of pulleys in the resin bath were varied in order to produce a longer impregnation time. The grooves in the pulleys were modified to encourage spreading of the yarn. Greater care was taken to insure complete solvent removal from the prepreg tape by drying the tape in a vacuum oven. Two tapes were prepared by dry winding the fiber, then painting with resin: numbers 21 and 23. All other tapes were impregnated in a wet winding technique.

A sample from each specimen was polished and examined microscopically. Based on that examination, selected specimens were submitted for flexural and short beam shear testing. The conditions utilized in Ref. 1 for Thornel 300/ P-1700 polysulfone were similar to those of run number 2 except the pressure was 6.9 MPa. Figure 1 is a photomicrograph of the baseline specimen of

HMS/P-1700 polysulfone using the Ref. 1 conditions, and shows high degree of porosity. This porosity is substantially greater than observed with the T300 composites and may be due to a greater difficulty in the resin penetrating the larger HMS tow.

One path which was explored to reduce this porosity was to use a more dilute solution thereby lowering the viscosity and improving the chances of the resin fully penetrating the bundle. It was demonstrated that the 7.5% resin solutions did not provide sufficient resin in the composite, and at least an 8.7% solution was necessary. The effect of the lower concentration is shown in Fig. 2. It was also shown that the application of greater pressure, as in numbers 19 and 22 where the latter was hot pressed at a pressure five times higher than the former, did not improve the microstructure of the composite as illustrated in Fig. 3.

Fairly good bundle penetration was obtained with the dry winding and hand painting technique employed in composites 21 and 23 as shown in Fig. 4. This possibly resulted from applying the resin to the tow while it was spread out on the drum and/or the penetration/separation which resulted from the brushing operation. This technique is much more time consuming than the wet winding process and does not lend itself to larger scale operations. Consequently, it was felt to be desirable to achieve better infiltration with the wet winding process.

The series of composites beginning with number 29 and running through 38 was primarily intended to explore the possibility that the porosity was due to entrapped solvent which was not fully removed from the impregnated tape prior to hot pressing. This had encouraging results in that several of the composites had lower porosity than earlier ones. In particular, specimens 32 and 34 shown in Fig. 5 had the best microstructures of any of the polysulfone matrix composites examined to that date. Both exhibited areas which were void free but also had some bundles with internal porosity.

A modification of the tape making process was initiated with composite 39. In order to reduce the tension in the yarn during the impregnation process and thereby improve the degree of infiltration, a driven roller was placed in line just before the impregnation bath. The speed of the roller was adjusted to produce nearly the same circumferential velocity as the take-up drum which resulted in very low yarn tension between the two. The rollers were covered with soft foam rubber to produce the necessary friction to drive the fiber bundle without abrading it.

Microscopic examination of the composites indicated that the two drive system tended to make the microstructures more uniform than in the past and that the overall porosity levels were somewhat reduced. However, it was found that composites which were hot pressed for short time periods (2-5 min) still possessed some porosity as in Fig. 6 which shows the specimen from trial 40. Longer duration hot pressing cycles were evaluated (nos. 43 and 44) and in both instances void content was substantially reduced. Microscopic observation revealed sporadic porosity in the bundle centers of the composite pressed for 30 min, and no porosity in the composite pressed for 60 min. Apparently the longer period allowed sufficient time for the resin to flow internally and fill the voids within the bundles. Figure 7 shows the microstructures of the two composites.

In addition to microscopic examination, several of the composites were tested to determine their flexural strength and modulus and short beam shear strength. These results are given in Table II. The values listed are averages of tests which were conducted in triplicate. An important point regarding the test data was brought out early in the program. The first three composites in Table II had microstructures which were very similar yet the average flexural strength of number 5, which was pressed at 315°C and 3.4 MN/m^2, was nearly 50% greater than that of the others. Thus the effects of hot pressing conditions must be explored in addition to optimizing impregnation procedure through microscopic observation. It is also of interest that composites 2 and 7 had the same strength, even though 2 was pressed at 0.7 MN/m^2 (100 psi) while 7 was pressed at 6.9 MN/m^2 (1000 psi). This implies that low pressure processing may be quite reasonable for the P-1700 polysulfone composites although this was not further explored in this program.

Composites 18 and 20 had high flexural properties but this was probably due to high fiber volume fractions which resulted from wet winding through a relatively dilute solution. The flexural moduli, in particular, reflected the high fiber content. Composites 21 and 23 were also impregnated with dilute solutions but in both instances a predetermined amount was applied by the painting technique and the fiber content appeared to be somewhat lower than that of most of the composites. The flexural properties of composites 32 and 34 were surprisingly low in view of their good microstructures.

On the basis of flexural and shear properties alone it was difficult to pinpoint those fabrication variables which were critical. Many of the composites which had good mechanical properties had very little in common in terms of fabrication procedures. Furthermore, there was frequently very little correlation between the measured properties and the quality of the composites as determined by microscopic observation. Both composites which were pressed for longer cycles had good combinations of properties, although not significantly better than some of the previous materials pressed for much shorter time periods.

However, the much better microstructure of composite 44 in particular indicated the likelihood of greater reproducibility, and as a result, the longer hot press cycle (60 min at 315°C, 3.4 MPa) was selected for Task II.

2.2.2 Polyethersulfone Matrix Composites

From a chronological standpoint much of the work on the polyethersulfone and polyarylsulfone composites followed that of the polysulfone matrix composites. As a result many of the impregnation technique refinements developed for the polysulfone tape preparation were incorporated into the process for making polyethersulfone and polyarylsulfone tape, and fewer fabrication trials were needed in the optimization process.

Table III lists the conditions used in the fabrication of HMS graphite composites having 300P polyethersulfone as the matrix. The first four trials were directed toward examining the effect of consolidation temperature and pressure. Photomicrographs of trials 1 and 4 which cover the condition extremes are presented in Fig. 8. In addition to the obvious porosity the composites appeared to be low in resin content and the resin concentration in the impregnating solution was increased in the succeeding trials.

Microscopic study of composites 5 through 9 indicated that many specimens had extensive porosity in the spaces between the bundles as can be seen in Fig. 9 for composite 7. This was substantially overcome through the use of the 4 hr at 150°C tape drying which was initiated with composite 10. The increased solids content in the impregnating solution also had a beneficial effect on the voids between bundles, but as indicated in Fig. 10, porosity still remained within the bundles.

The final optimization came about by utilizing the driven roller prior to impregnation (no. 14), increasing the resin content in the impregnating solution to 12.5% (no. 16), and by hot pressing for 60 minutes. This resulted in a nearly void-free microstructure as shown in Fig. 11 which is a photomicrograph of composite 20. Although some porosity is evident in the bundle centers in Fig. 11, much of the composite was totally free of voids.

The results of the mechanical tests on the polyethersulfone matrix composites are given in Table IV. Contrary to the experience with the P-1700 polysulfone composites, there was a definite correlation between the observed quality of the composite and its properties, especially the short beam shear strength. Composite 20 clearly had the best combination of flexural properties, shear strength, and microstructure, and as a result, the impregnation/consolidation cycle used in its fabrication was selected for Task II.

2.2.3 Polyarylsulfone Matrix Composites

Unlike the other two thermoplastics investigated in the program, polyarylsulfone does not form a true solution. With the DMF solvent, it forms a stable suspension, and as a result of sieving the powder as described earlier the small particles of resin were capable of penetrating the graphite fiber bundles to a substantial degree. However, complete infiltration of the bundles remained a problem throughout this phase of the program and never was satisfactorily achieved.

The fabrication variations investigated with Astrel 360 matrix composites are given in Table V and the mechanical properties measured on selected laminates are given in Table VI. The conditions listed for fabrication trial 1 were the same as those used in the fabrication of polyarylsulfone matrix composites in Ref. 1. The photomicrograph of the specimen, shown in Fig. 12, indicates the porosity in the center of the filament bundles. Initial variation in drying time (Fig. 13) and temperature/pressure combination in hot pressing (Fig. 14) established the apparent need for a long drying cycle and a high hot pressing temperature. However, the longer drying cycle used in trial no. 2 did not result in a significant improvement in void content as indicated in Fig. 13, and the desirability of a high hot pressing temperature was concluded because of the poorer results shown in Fig. 14 for fabrication trials 5 and 6.

Beginning with trial no. 8 effort was primarily directed to examining variations of a high pressure/high temperature consolidation with a constant tape drying cycle. Trial no. 8 represented a reasonable improvement in void content as indicated in Fig. 15, however, the other trials conducted with a 5 minute pressing showed no additional reduction in void content. As with the other materials, the best results occurred with a longer consolidation cycle. Figure 16 is a photomicrograph of the composite which resulted from fabrication trial 14 in which a 60 minute hot press time was used. Although there was still a reasonably large amount of porosity in the center of the bundle, further effort with this system did not seem warranted in view of the consistently lower properties which were measured (Table VI) throughout the trials and the inherent impregnation problem caused by a lack of solubility of the resin. Although the elevated temperature performance of the Astrel 360 composites was demonstrated in Ref. 1 to be better than that of P-1700 polysulfone and literature data indicated it to be better than that of the 300P polyethersulfone, its maximum use temperature was substantially in excess of that required in the fan exit guide vane to be evaluated in Task III. The poorer ambient performance of the material made it an unlikely choice for Task III and therefore further effort to reduce void content was felt unjustified. As a result, the conditions of fabrication trial 14 were selected for Task II work.

3.0 TASK II - MECHANICAL PROPERTIES EVALUATION

The objective of Task II was to provide mechanical property data on composites having each of the three thermoplastic resins as matrix. Static properties, pendulum impact properties, and stress-rupture properties were to be measured as a function of temperature in order to assess the maximum use temperature of each material. Also, the effects of hybrid reinforcement were to be evaluated and one of the materials was to be tested in bending fatigue.

3.1 Experimental Procedure

3.1.1 Test Plan

The test plan for Task II is summarized in Table VII. The program was designed to compare the pertinent properties of each composite system with particular emphasis on those properties which are most sensitive to matrix effects and/or matrix-fiber interfacial strength. Elevated temperatures for the flexural, shear, impact, and tensile testing were selected based on past experience to bracket the upper use temperature of each system. Temperatures for the stress-rupture testing were selected based on the results of the static tension tests.

3.1.2 Materials

All resins and the graphite reinforcement were the same as those used in Task I. The hybrid composites were made with the HMS graphite in combination with 12 end S-glass roving.

3.1.3 Fabrication

The fabrication procedures for each resin system were selected based on the results of Task I as discussed previously. The conditions are summarized below:

Matrix	Resin wt %	Solvent	Tape Dry	Hot Pressing Temp °C	Hot Pressing Time (min)	Hot Pressing Pressure MPa
P-1700 Polysulfone	10	methylene chloride	4 hrs at 150°C in air	315	60	3.4
300P Polyethersulfone	12.5	dimethyl-formamide	4 hrs at 150°C in air	315	60	13.8
Astrel 360 Polyarylsulfone	11	dimethyl-formamide	4 hrs at 150°C in air	370	60	13.8

Hybrid composites were an intraply combination of graphite and glass. All impregnation/fabrication procedures were the same as those used for the all-graphite composites except the winding involved alternating graphite and glass tows across the width of the tape. This was accomplished by first winding the graphite at a greater than usual spacing, then winding the glass in the spaces between the graphite bundles.

3.1.4 Test Techniques

Short beam shear and flexural tests were performed in the same manner as in Task I. Tensile specimens were 15.2 cm long x 1.25 cm wide in the gage section and 1.9 cm wide in the shoulder for gripping. Nominal thickness was .25 cm. Pendulum impact tests were conducted on "thin" specimens which were 5.5 cm x 1 cm wide x .25 cm thick with no notch. The test was of the "Charpy" type with instrumentation to provide a load vs time trace for each specimen. Stress-rupture testing was performed using specimens of the same geometry as described for the tensile test. The apparatus was equipped with a timer which recorded failure to the nearest tenth of an hour.

3.2 Results and Discussion

3.2.1 P-1700 Polysulfone Composites

The mechanical properties measured on HMS/P-1700 polysulfone composites are listed in Table VIII. The unidirectional flexural and $\pm 45°$ tensile data clearly indicated that the material had lost a substantial fraction of its room temperature capability at 149°C. The short beam shear strength dropped more severely at 163°C, and the pendulum impact data, both energy absorbed and load carrying ability, were essentially independent of test temperature. The room temperature

flexural and shear strength properties of the material were somewhat higher than those measured in Task I on the composite fabricated under the optimized conditions. Retention of these properties at 122°C was good.

Representative results of the instrumented pendulum tests are shown in Fig. 17 for each of the test temperatures. In addition to the load-time trace, a cumulative energy trace was produced during each test. The scales given for the room temperature (22°C) load and time axes also apply to the curves obtained at the elevated temperatures. As the energy and maximum load data in Table VIII indicate there was very little effect of temperature on the response of the material. The only noticeable difference of any significance was the longer time of unloading of the specimen tested at 163°C which in turn resulted in somewhat higher energy absorbed at that temperature. This was due to the softening of the resin which was observed in the static mechanical tests at lower temperatures. The high load carrying ability at 163°C in the impact test demonstrated the effect of higher strain rate testing.

The tensile tests of laminates in a $\pm 45°$ configuration showed that the material did not have structural capability at 163°C. As a result stress-rupture tests were carried out at the 122°C and 149°C temperatures. The data from the tests are presented in Figs. 18 and 19 in terms of initial stress versus time at that stress. Darkened symbols indicate failure, while open symbols indicate no failure. Different symbols (triangles, circles, squares) indicate different laminates from which the specimens were cut. This latter indication was made because some of the laminates produced lower strength specimens than others; in particular the laminate used to measure the static properties shown by the triangles was of low strength. This was unfortunate because it resulted in several runouts at the 100 hour period of interest since stress levels were based on static strengths. This was especially true for the 122°C tests. Nevertheless enough tests were conducted to obtain good estimates of the 100 hour stress-rupture limits. At 122°C a stress of approximately 69 MPa (10 ksi) could be sustained for 100 hrs, while at 149°C the comparable stress was 29 MPa (4.3 ksi).

The data obtained from testing the HMS/glass/P-1700 polysulfone hybrids are listed in Table IX. In all cases the static strengths and moduli were lower than those of the all graphite composites. While the lower moduli were not unexpected, the decreased shear and flexural strengths were somewhat surprising. However, the shear strength still compares very favorably with published results for HMS/epoxy of 49 MPa (7.1 ksi) (Ref. 2), and the flexural strength and modulus are believed sufficient for many applications. The primary advantage of hybrids is the substantial increase in energy absorbed during fracture and this was verified for the HMS/glass/P-1700 composites. The energy results in Table IX and the load-time curves in Fig. 20 indicate a factor of three to four improvement in the fracture energy per unit area. However, as pointed out in Ref. 2, the load carrying ability

of hybrids in this type of test is generally the same as or lower than that of an unhybridized composite. This conclusion was also verified by the results of this study which showed that the load carrying abilities of the two systems were about equal at room temperature and the graphite/polysulfone was better at the 122°C test temperature.

3.2.2 300P Polyethersulfone Composites

The mechanical properties of the HMS/300P polyethersulfone composites are given in Table X. Although there was a substantial drop in flexural strength at 149°C from the room temperature values, useful strength properties were retained to at least 177°C. The flexural modulus at 177°C was only 10-15% lower than the room temperature modulus. Short beam shear strength followed the same trend as the flexural strength although the drop-off at 149°C was not as severe.

As with the P-1700 polysulfone composites, test temperature did not have too significant an effect on the pendulum impact behavior of the polyethersulfone matrix composites. The energy, in particular, was insensitive to temperature, and with the exception of one value at 22°C which was high, and one value at 204°C which was low, the energy per unit area was essentially constant. The maximum loads did drop off at the two highest test temperatures and the load-time curves exhibited a nonlinearity at the point of maximum load as shown in Fig. 21. This nonlinearity was probably the result of local deformation at the point of impact rather than general yielding of the matrix throughout the composite. Tested specimens exhibited a "dent" where the tup struck.

The tensile tests of the $\pm 45^{\circ}$ laminates produced even more scatter in strength than the P-1700 polysulfone matrix. With the exception of the 177°C tests there was a large variation in strength among the three specimens tested at a given temperature. Although the reasons for this are not clear, the variation may have been due to machining-induced defects in the specimens since there were some inconsistencies noted in the edges, especially in the region of the shoulder radius. The materials were judged to have good property retention up to 177°C, and that temperature and 149°C were selected for stress-rupture testing.

Stress-rupture test results for the 149°C and 177°C conditions are given in Figs. 22 and 23, respectively. Although there was a large variation in the static tests at 149°C, the stress-rupture results were relatively consistent, and the data indicated a 100 hr stress limit of approximately 69 MPa (10 ksi) at that temperature. As shown in Fig. 23 the 100 hr stress at 177°C was 62 MPa (9 ksi) or nearly as high as the 149°C value. These results demonstrated a significantly higher upper use temperature for the 300P polyethersulfone than that which was found for the P-1700 polysulfone matrix composites.

3.2.3 Astrel 360 Polyarylsulfone Composites

The results of the tests performed on the HMS/Astrel 360 polyarylsulfone composites are given in Table XI. The flexural and shear strengths were lower than the values measured in the optimization work during Task I which emphasizes the problem of achieving repeatable results with a system in which complete resin impregnation of the fiber bundle is not achieved. The elevated temperature testing revealed excellent retention of properties up to 204°C with some drop-off at 232°C. However, even though the retention of the polyarylsulfone composites was good, the polyethersulfone composites had better absolute strengths at 204°C.

The thin pendulum impact behavior of the polyarylsulfone composites was completely insensitive to test temperature in terms of both energy absorbed and load carrying ability. Figure 24 which shows representative load-time traces for tests carried out at each temperature indicates the similarity of behavior.

The $\pm 45°$ tensile results showed no change in strength with temperature but did exhibit a decrease in modulus at the lowest elevated temperature (177°C), then a constant value at the other elevated test temperatures. This consistent performance was also reflected in the stress-rupture behavior as shown in Figs. 25 and 26. At both 177°C and 204°C the $\pm 45°$ specimens were capable of withstanding a stress of approximately 43 MPa (6.2 ksi) without rupture for 100 hrs.

3.2.4 Fatigue Testing

Based on the evaluation of composite properties as a function of temperature as discussed above, an assessment of the temperature requirements for the composite fan exit guide vane, and the ease of processing each system, polyethersulfone was selected for Task III vane fabrication and Task II fatigue studies.

The specimen test conditions for the fatigue study are listed in Table XII. In general the number of cycles each specimen was subjected to was determined by the change in stiffness which was measured during the course of the testing. A 25% reduction in either bending or torsional stiffness was used as a criterion for terminating the tests.

A typical result is illustrated in Fig. 27 for specimen 33-1 which was subjected to an alternating stress of 318 MPa (46 ksi) for 10^7 cycles. Although there was some scatter in the measurements, the torsional rigidity exhibited a steady decrease after approximately 10^5 cycles. The stiffness had dropped to 90% of its original value after 1×10^6 cycles, and to 80% of its original value after 1×10^7 cycles. The loss in stiffness was due to the formation of shear cracks which were frequently visible with the naked eye. The cracks usually

initiated in or near the fixed grips in the fatigue test and their effect on bending stiffness was much less predictable, depending on whether they extended into the grips in the stiffness retention test. Consequently, torsional stiffness loss alone was utilized as a measure of failure.

After plotting the data for each specimen as in Fig. 27, the number of cycles for 100%, 90%, and 80% retention of torsional stiffness was determined then compiled into an S-N plot in Fig. 28 for all specimens. The data points are shown for each curve and it is clear that a good deal of scatter existed. Furthermore, the unknown influence of possible stress concentrations during testing caused by the grips leads to the conclusion that the fatigue data must be considered as preliminary. Results more meaningful for the vane application were generated in Task III.

4.0 TASK III - HARDWARE FABRICATION AND EVALUATION

The objectives of Task III were to demonstrate the feasibility of fabricating fan exit guide vanes from graphite/thermoplastic composites and to compare the stiffness, frequency, and fatigue response of such vanes to that of similar vanes fabricated from graphite/epoxy composite.

4.1 Experimental Procedure

4.1.1 Test Plan

Five HMS graphite/300P polyethersulfone fan exit guide vanes were to be fabricated by the Commercial Products Division of Pratt & Whitney Aircraft Group using prepreg prepared by United Technologies Research Center. The vanes were to be tested nondestructively to measure spring rates, then three were to be destructively fatigue tested with primary attention devoted to the stresses generated at the trailing edge of the vanes. All testing was conducted at P&WA/CPD.

4.1.2 Materials

HMS/300P polyethersulfone was used for all vanes. Impregnation procedures were identical to those used in Task II.

4.1.3 Fabrication

The first step in the fabrication procedure was prepreg preparation which was accomplished using established techniques. In order to aid in vane layup, steps were taken to insure the prepreg was relatively flat. Once solvent has been removed, the tape has no tack, and if dried on the windup drum, will retain the curvature of the drum to some extent. In order to flatten the tape, it was partially dried on the drum for 20 minutes with a heat gun, then removed from the drum and laid on a table to dry under ambient conditions. Final drying was done at 150°C for four hours on an oven shelf.

Ply design for the vanes consisted of using the known thickness per ply of the composite and the established vane envelope. Since the vane has a constant cross section along its span, only chord-wise ply drop-offs were necessary. The final ply configuration consisted of a $\pm 35^{\circ}$ shell (2 plies) which extended full chord and an inner core of 0° plies which was 15 layers thick at mid chord.

The sequence of operations in the fabrication of a vane is shown in Fig. 29. The first step shows the package being assembled. Since the prepreg had no tack, the layers were held together by spot heating and locally melting the resin. This technique was found to be more satisfactory than solvent bonding which was much slower and left residual solvent to be removed. The second photograph shows a completed ply package. In order to facilitate handling and to minimize the possibility of misalignment or shifting of the plies, the layup was next subjected to a preforming operation depicted in the third photograph. The plies were inserted between two metal sheets which were bent to a curvature which approximated the camber of the vane. Pressure was applied by clamping, then the assembly was placed in an oven at 285°C for 20 minutes. The fourth picture shows a preformed vane with an aluminum leading strip in position for final molding. The final molding cycle deviated slightly from that used in the previous portions of the program due to limitations of the press used. The intended conditions were 370°C for 60 minutes at a pressure of 13.8 MPa, but the maximum pressure capacity of the press was 8.2 MPa for a part the size of the vane. However, this cycle proved to be completely satisfactory and good flow of the resin was achieved as illustrated in the fifth picture in Fig. 29 which shows both sides of a vane after removal from the mold. After a minor trimming of flash around the edges the finished vane is shown in the final photograph in the figure.

4.1.4 Test Techniques

Bending spring rate was determined by supporting the vane at the ends on two knife edges and then loading the vane along the concave surface. The load was applied over a major portion of the vane span by using a pressurized bladder, thereby simulating the aerodynamic loading the vane would experience in the engine. The use of this approach is important, since the spring rate of the vane is influenced by vane deflected shape, including the degree of uncamber produced by the aerodynamic loading. Dial indicators were used to document the response of the vane to the loading.

Torsional spring rate was determined by clamping one end of the vane in a vertical stand and applying a pure torque on the opposite end while measuring the deflection with dial indicators. The clamps are contoured to ensure that clamping does not distort the vane camber.

Fatigue testing was conducted on an electrodynamic exciter that excited the vane in the first bending mode. The dynamic excitation was superimposed on a uniform bending static load to simulate engine aerodynamic loading.

In order to properly mount and align the vane in the test fixture it was necessary to bond in place silicone rubber feet as shown in Fig. 30. The silicone was poured into the hollow aluminum cylinders into which the vane had been previously inserted and accurately positioned.

The test fixture is shown in Fig. 31. As shown, the vane is equipped with rubber feet that ride on the two supporting rollers. Rotation of these rollers bows the vane, producing the desired static load. The degree of loading was determined by a strain gage located at the midspan location of the concave surface at the vane trailing edge. Previous experience indicated that this location is the critical stress location during fatigue testing. The precise strain levels used were determined on the basis of the design analysis and the results of prior testing. Initially, however, the static strain was expected to be in the range of -3000 microinches/inch compression. The dynamic strain was to be progressively increased, beginning at 1200 microinches per inch and then increased by 200 microinches per inch every 10^7 fatigue cycles until failure occurred.

4.2 Results and Discussion

The results of the spring rate testing of the five vanes are given in Table XIII. These values were about a factor of three higher than those of the former bill of material graphite/epoxy vanes. For example, the bending spring rate of the B/M vanes was approximately 1000 lbs/in. A portion of the increased stiffness of the current vanes could be attributed to the fact that they were somewhat thicker than the nominal dimension of the B/M vane. Without polyurethane coating the maximum nominal thickness was .52 cm (.205 in.) while the polyethersulfone matrix vanes were approximately .56 cm (.220 in.). However, since the finished B/M vanes had a .025 cm (.01 in.) coating of polyurethane coating on both surfaces, the polyethersulfone matrix vanes were under the specified final vane thickness. In any event the increase of 10% in overall thickness should have caused an increase in section modulus of approximately 35% rather than the 300% increase in stiffness which was observed. Additional factors which may have contributed to the higher spring rates are higher fiber volume fraction, higher fiber modulus, different ratio of shell angle plies to core 0° plies, and better overall quality resulting in more optimum fiber distribution.

Due to the much greater stiffness of the vanes the fatigue conditions were modified in order to produce loads similar to those which would occur in an engine. Table XIV summarizes the fatigue histories of the three vanes which were tested. The previous history of testing vanes indicated that those vanes which could withstand a steady strain of -3000 μin/in (compression) $\pm$ 2400 μin/in in the span-wise direction at midspan on the trailing edge would perform satisfactorily in an engine under the most severe operating conditions. This translated to -1000 μin/in $\pm$ 800 μin/in for the stiffer vanes.

The first vane tested, XKT 1175-8, was started at a lower dynamic stress and run-out before reaching the critical conditions. After also passing the next level with no evidence of failure, the dynamic stress was further increased,

finally to the capacity of the test machine, and the steady stress was also increased. Failure finally occurred in the trailing edge after 8.3×10^6 cycles at -1500 μin/in ± 1600 μin/in. These conditions represented 150% of the steady load and 200% of the dynamic load of the bill of material vanes and are more severe than any endured by the best of the former vanes. Figure 32 shows the failure, a delamination at the trailing edge, which is typical of the mode which was observed in previous testing.

The second vane tested, XKT 1175-9, was begun at much higher strain levels and demonstrated an endurance very similar to that of the first vane. The third vane appeared to have failed under less severe conditions, -1500 μin/in ± 1400 μin/in, however the chordwise strain gage at midspan on the trailing edge indicated a dynamic strain approximately 80% greater than that read out for the spanwise direction. Usually the strains in the two directions at that location are approximately equal. The reason for the higher chordwise strain in this instance is not known but it might be related to a disbond which was observed between one of the rubber feet and the vane which in turn produced an unusual state of stress during the test. In any event the apparent premature failure was probably related to the high chordwise stress, and in general the three thermoplastic matrix vanes exhibited excellent fatigue performance.

5.0 CONCLUSIONS

Based on the results of this program the following conclusions were reached:

1. HMS graphite reinforced P-1700 polysulfone and 300P polyethersulfone composites can be processed to have very low void content and good mechanical properties at ambient temperature.

2. Astrel 360 polyarylsulfone is much more difficult to process into a good quality composite because of its poor solubility.

3. Substantial drop-off of short term static properties occurred at the following temperatures:

P-1700 polysulfone	149°C
300P polyethersulfone	177°C
Astrel 360 polyarylsulfone	>232°C

4. 100 Hour stress-rupture tests indicated the same upper use temperature limits as the short term tests.

5. Over the temperature range investigated, all three composite systems exhibited thin pendulum impact behavior which was essentially independent of test temperature.

6. Bending fatigue behavior of HMS graphite/300P polyethersulfone was characterized by noncatastrophic shear failure which resulted in a gradual loss of composite stiffness.

7. Fan exit guide vanes were successfully fabricated from HMS graphite/300P polyethersulfone. These vanes had bending spring rates approximately three times higher than those of graphite/epoxy vanes which were formerly bill-of-material. The fatigue performance of the HMS/300P vanes was better than that of any of the standard graphite/epoxy vanes previously tested.

ACKNOWLEDGEMENT

The author wishes to acknowledge the efforts of Dr. A. J. Dennis of the Commercial Products Division of Pratt & Whitney Aircraft Group who coordinated the vane fabrication and testing activities carried out by his organization.

REFERENCES

1. R. C. Novak: "Graphite Fiber Reinforced Thermoplastic Resins", NASA CR-134881, July 1975.

2. R. A. Pike and R. C. Novak: "Design, Fabrication and Test of Multi-Fiber Laminates", NASA CR-134763, January 1975.

Table I

Fabrication Parameters with Polysulfone Resin

No.	Fiber	Resin wt %	Solvent[1]	Winding Conditions: Speed (m/min)	Winding Conditions: Pulleys	Winding Conditions: Tape Dry	Pressing Conditions: Temp (°C)	Pressing Conditions: Time (min)	Pressing Conditions: Pressure MPa	Notes
2	HMS	10	M.C.	11.5	1	air	270	5	0.7	
3							315		0.7	
4							315		6.9	
5							315		3.4	
6							270		3.4	
7							270		6.9	
8		11								
9		11				heat gun				
10		10			2	air				
11										
12										
13			M.C.+T.C.							wetting agent
14										
15		7.5								
16										wetting agent
17										
18	HMU	8.7								
19	HMS					80°C vac.				
20				4.5						
21				11.5						wound dry, painted
22									34.5	wetting agent
23									34.5	wound dry, painted
24		7.5							6.9	
25		10							6.9	wetting agent
26			M.C.						6.9	wetting agent
27							315		3.4	wetting agent
28				4.5					3.4	wetting agent, rollers
29				6		150°C vac.			3.4	wetting agent
30									1.4	
31							308		5.2	
32						115°C vac.	315		6.9	
33							315		3.4	
34							343	2		
35							343	2		
36						343°C air	343	2		
37						150°C air	315	5		
38						115°C vac.				
39						150°C air				
40										
41										
42						150°C vac				
43						150°C air		30		
44						150°C air		60		

[1]M.C. = methylene chloride; T.C. = trichloroethylene

Table II

Mechanical Properties of Unidirectional
Polysulfone Matrix Composites

No.	Flexural Properties				Shear Strength	
	Strength		Modulus			
	MPa	ksi	GPa	msi	MPa	ksi
2	647	94	159	23.0	32	4.7
5	998	145	168	24.3	57	8.3
7	704	102	170	24.6	29	4.1
18	1198	174	209	30.3	60	8.6
20	942	137	185	27.2	38	5.5
21	772	112	150	21.8	39	5.7
23	931	135	139	20.2	55	8.0
27	1014	147	161	23.3	55	8.0
29	967	143	180	26.2	65	9.4
32	872	127	167	24.2	53	7.6
34	808	118	162	23.4	53	7.7
40	874	127	164	23.7	39	5.7
41	847	122	165	24.0	49	7.2
43	930	135	185	26.9	60	8.7
44	970	141	192	27.8	68	9.6

Table III

Fabrication Parameters with Polyethersulfone

No.	Resin Wt %	Solvent	Wind Speed (m/min)	Tape Dry	Pressing Conditions			Wetting Agent	Notes
					Temp (°C)	Time (min)	Pressure MPa		
1	10	DMF	6	150°C vac 1 hr	315	5	13.8	-	
2	10				315		13.8	NP-14	
3	10				343		13.8		
4	10				370		6.9		
5	11				343		13.8		paint
6	11			150°C air 1 hr vac 16 hrs	343		13.8		paint
7	11				343		13.8		
8	11				343		13.8		
9	11			150°C air 16 hrs	315		6.9		
10	11			150°C air 4 hrs	315		6.9		
11	12				260		6.9		
12	12				260		13.8		
13	12				315		6.9		
14	11				343		13.8		
15	11				343		3.4		
16	12.5				315		6.9		
17	12.5						13.8		
18	12.5						13.8		
19	12.5					30	13.8		
20	12.5					60	13.8		

Table IV

Mechanical Properties of Unidirectional
Polyethersulfone Matrix Composites

No.	Flexural Properties				Shear Strength	
	Strength		Modulus			
	MPa	ksi	GPa	msi	MPa	ksi
2	949	138	201	29.1	51	7.4
3	1135	165	205	29.7	48	7.0
7	1130	164	204	29.6	56	8.2
10	1082	157	173	25.1	56	8.2
12	665	96	139	20.2	40	5.8
13	1080	156	186	27.0	51	7.3
14	1160	168	193	27.9	49	7.1
15	1250	181	192	27.8	-	-
16	1290	186	197	28.6	54	7.9
17	854	124	182	26.4	75	10.8
19	1240	180	203	29.5	74	11.7
20	1360	198	210	30.0	80	11.7

Table V

Fabrication Parameters with Polyarylsulfone

No.	Resin Wt %	Solvent	Wind Speed (m/min)	Tape Dry	Pressing Conditions			Wetting Agent
					Temp (°C)	Time (min)	Pressure MPa	
1	10	DMF	6	150°C 1 hr air 16 hr vac	370	5	6.9	NP-14
2				150°C 4 hr air	370		6.9	
3				150°C 4 hr air	343		6.9	
4				150°C 1 hr air	315		13.8	
5				150°C 1 hr air	343		13.8	
6				150°C 4 hr air	315		13.8	
7					370		6.9	
8					370		13.8	
9					370		35	
10	11				343		13.8	
11					315			
12					370			
13					370	30		
14					370	60		

Table VI

Mechanical Properties of Unidirectional
Polyarylsulfone Matrix Composites

No.	Flexural Properties				Shear Strength	
	Strength		Modulus			
	MPa	ksi	GPa	msi	MPa	ksi
1	1007	146	180	26.1	41	6.0
2	1096	159	183	26.5	38	5.4
5	160	23	118	17.1	12	1.7
9	739	107	161	23.4	41	5.9
12	1080	158	188	27.3	42	6.1
14	965	140	183	26.5		

Table VII

Task II Test Plan

Matrix	Reinforcement	Test	Test Temperatures (°C)	Ply Configuration
P-1700 Polysulfone	HMS	Flex, Shear, Impact	22, 122, 149, 163	0
		Tension	"	±45
		Stress-rupture	select	±45
	HMS/Glass	Flex, Shear, Impact	22, 122	0
		Tension	22, 122	±45
300P Polyethersulfone	HMS	Flex, Shear, Impact	22, 149, 177, 204	0
		Tension	"	±45
		Stress-rupture	select	±45
Astrel 360 Polyarylsulfone	HMS	Flex, Shear, Impact	22, 177, 204, 232	0
		Tension	"	±45
		Stress-rupture	select	±45
Select	HMS	Bending Fatigue	22	0

Table VIII

HMS/P-1700 Polysulfone Mechanical Properties

Test Temp °C	Unidirectional Flexural Strength ksi	MPa	Unidirectional Flexural Modulus msi	GPa	Unidirectional Shear Strength ksi	MPa	Unidirectional Impact Energy ft-lbs/in^2	j/cm^2	P_{max} lbs	KN	±45° Tension Strength ksi	MPa	Modulus msi	GPa
22	155	1070	25.9	179	10.2	70	19.2	4.02	250	1.12	14.8	102	2.6	18
	163	1020	26.4	182	9.9	68	20.0	4.20	240	1.11	11.0	76	3.4	23
	168	1160	27.6	190	9.3	64	16.6	3.51	250	1.12	9.8	68	2.3	16
122	140	965	23.8	164	7.1	49	15.6	3.28	220	.98	9.6	66	2.1	14
	129	889	23.3	161	7.1	49	18.7	3.91	240	1.09	7.5	52	1.7	12
	127	876	26.2	181	6.7	46	17.1	3.60	260	1.16	6.4	44	1.6	11
149	35	240	8.4	58	5.0	33	18.7	3.92	240	1.05	4.2	29	0.8	5
	55	380	11.3	78	5.1	35	18.0	3.78	210	.94	3.2	22	1.3	9
					5.1	35	17.0	3.59	210	.94				
163	11	78	4.2	29	2.3	16	20.3	4.27	230	1.02	0.7	5	0.4	3
	18	125	4.0	27	1.6	11	22.0	4.64	240	1.09				
	11	75	2.7	18	1.7	12	24.2	5.10	240	1.09				

Table IX

HMS/Glass/P-1700 Polysulfone Mechanical Properties

Test Temp °C	Unidirectional Flexural Strength ksi	MPa	Unidirectional Flexural Modulus msi	GPa	Unidirectional Shear Strength ksi	MPa	Unidirectional Impact Energy ft-lbs/in^2	j/cm^2	P_{max} lbs	KN
22	116	803	19.0	131	8.6	59	82.3	17.3	245	1.09
	122	842	18.7	129	8.6	59	81.8	17.2	228	1.01
	127	874	18.9	130	9.0	62	103.0	21.7	245	1.09
122	103	710	19.8	136	5.8	40	81.1	17.1	204	0.91
	97	669	19.2	133	6.2	43	78.8	16.6	204	0.91
	106	731	21.4	147	6.0	41	60.0	12.6	196	0.87

Table X

HMS/300P Polyethersulfone Mechanical Properties

Test Temp °C	Unidirectional Flexural Strength ksi	MPa	Unidirectional Flexural Modulus msi	GPa	Unidirectional Shear Strength ksi	MPa	Unidirectional Impact Energy ft-lbs/in^2	j/cm^2	P_{max} lbs	N	±45° Tension Strength ksi	MPa	Modulus msi	GPa
22	202	1390	27.4	189	9.9	68	13.5	2.84	210	920	12.1	83	5.0	34
	191	1320	27.5	190	10.6	73	14.1	2.94	180	780	21.5	148	4.0	28
	175	1200	27.1	187	11.2	77	26.0	5.46	170	740	12.9	89	5.4	37
149	122	845	27.0	187	9.1	62	13.7	2.89	160	710	19.6	135	3.0	21
	115	794	22.5	155	7.1	49	11.9	2.53	200	890	11.3	78	2.8	19
	126	870	20.9	144	7.0	48	12.6	2.66	160	710	16.9	117	2.8	19
177	112	771	23.7	163	6.6	46	13.6	2.86	150	670	11.9	82	2.5	17
	106	729	20.9	144	6.2	43	11.4	2.40	140	640	10.8	74	2.6	18
	103	714	23.1	159	6.7	46	14.8	3.10	150	670	13.4	92	2.3	16
204	97	666	17.9	123	5.8	40	13.6	2.87	140	640	1.2	8	0.2	1
	72	496	16.6	114	5.3	37	8.3	1.76	150	670	7.4	51	2.2	15
	58	402	20.2	139	5.9	40	12.3	2.61	140	640	9.8	68	1.1	8

Table XI

HMS/Astrel 360 Polyarylsulfone Mechanical Properties

Test Temp °C	Unidirectional Flexural Strength ksi	MPa	Unidirectional Flexural Modulus msi	GPa	Unidirectional Shear Strength ksi	MPa	Unidirectional Impact Energy ft-lbs/in^2	j/cm^2	P_{max} lbs	N	±45° Tension Strength ksi	MPa	Modulus msi	GPa
RT	52	360	18.4	127	4.3	30	21.7	4.56	114	511	7.5	52	4.5	31
	46	320	21.3	147	4.4	31	25.0	5.25	114	511	6.1	42	4.4	30
	61	420	23.1	159	4.6	32	22.8	4.79	98	439	8.0	55	5.8	40
177	53	370	22.7	157	4.3	30	21.2	4.46	98	439	8.4	58	2.3	16
	62	430	25.1	173	4.4	31	19.7	4.14	114	511	7.7	53	1.9	13
	47	320	22.0	152	4.7	32	21.3	4.47	114	511	7.6	52	2.1	14
204	27	180	25.2	174	4.5	31	22.0	4.62	98	439	7.9	54	2.0	14
	54	370	22.6	156	3.4	24	20.0	4.20	98	439	7.4	51	1.8	12
	54	370	20.7	143	4.1	28	19.7	4.14	98	439	8.3	57	1.8	12
232	38	260	20.0	138	3.3	23	22.2	4.67	106	575	10.0	69	1.3	9
	45	310	21.3	147	-	-	19.8	4.16	98	439	6.6	46	1.9	13
	44	300	20.4	140	3.3	23	22.3	4.69	98	439	6.6	46	1.7	12

Table XII

Fatigue Conditions

No.	Alternating Stress MPa	ksi	Number of Cycles
32-5	1040	151	3×10^4
32-6	918	133	4.5×10^4
32-7	1090	158	6×10^4
33-2	600	87	7.5×10^4
33-1	318	46	8.3×10^6
32-1	524	76	5.9×10^6
32-2	372	54	1×10^7
32-3	476	69	9.2×10^6
32-4	379	55	8.3×10^6

Table XIII

Vane Spring Rates

Number	Torsional Spring Rate		Bending Spring Rate	
	N·m/deg.	in-lb/deg	N/cm	lb/in
XKT 1175-5	2.47	21.0	3800	2171
XKT 1175-6	2.93	25.9	4660	2663
XKT 1175-7	3.25	28.8	5700	3257
XKT 1175-8	3.44	30.4	6070	3470
XKT 1175-9	3.04	26.9	5330	3046

Table XIV

Vane Fatigue Results

Number	Static Strain @ Trailing Edge (μcm/cm)	Dynamic Strain @ Trailing Edge (μcm/cm)	No. of Cycles
XKT 1175-8	-1000	600	10^7
	-1000	800	10^7
	-1000	1000	10^7
	-1000	1200	10^7
	-1000	1400	10^7
	-1500	1000	10^7
	-1500	1400	10^7
	-1500	1600	8.3×10^6
XKT 1175-9	-1500	1400	10^7
	-1500	1600	4.5×10^6
XKT 1175-7	-1500	1400	1×10^6

FIG. 1

HMS/P–1700 POLYSULFONE COMPOSITE MADE UNDER BASELINE CONDITIONS

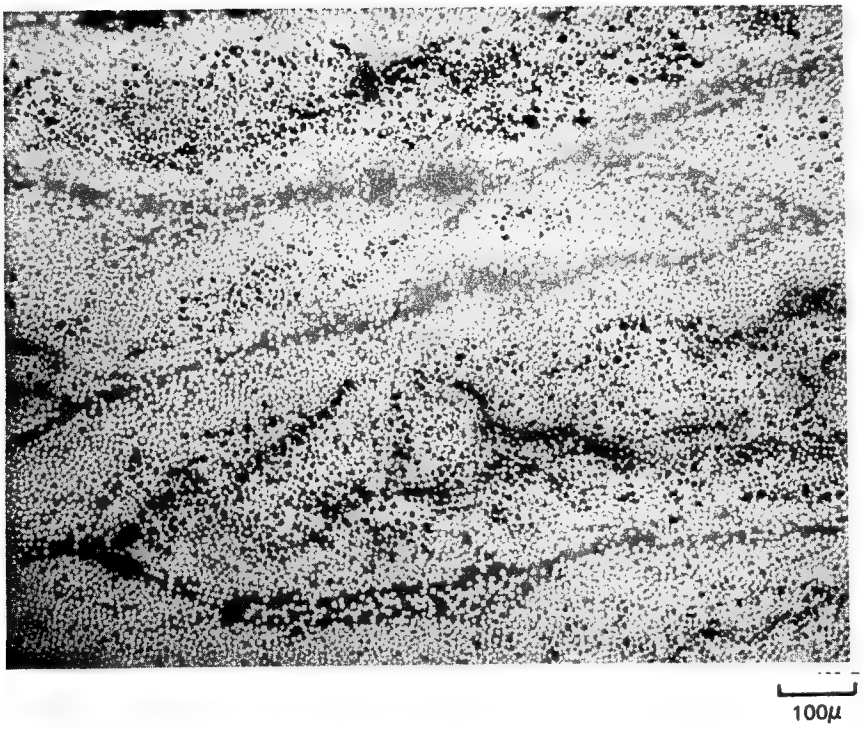

77–03–120–5

FIG. 2

HMS/P–1700 POLYSULFONE FROM 7.5% SOLUTION

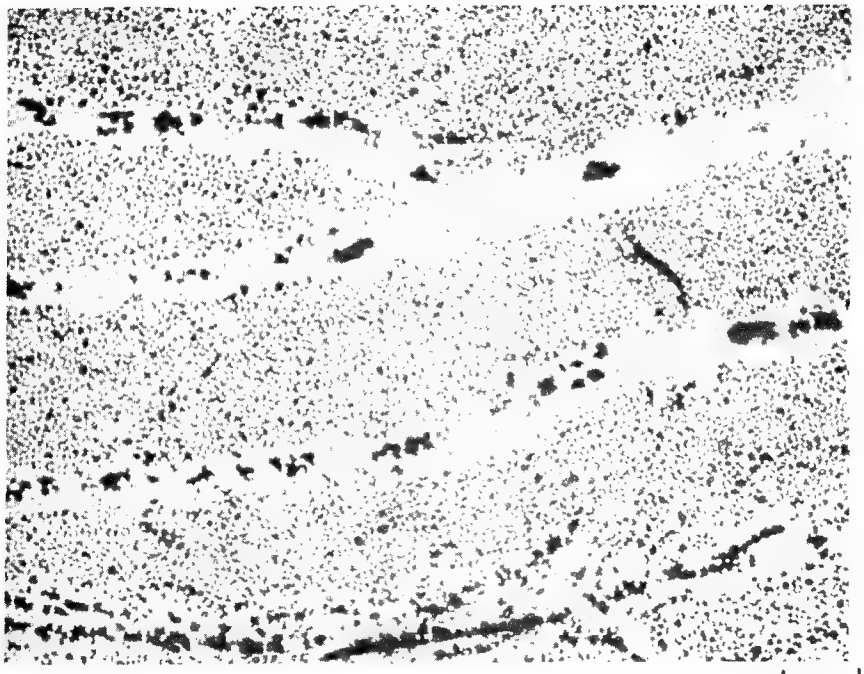

FABRICATION TRIAL NO. 16

100μ

77–03–120–4

EFFECT OF CONSOLIDATION PRESSURE ON HMS/P–1700 POLYSULFONE

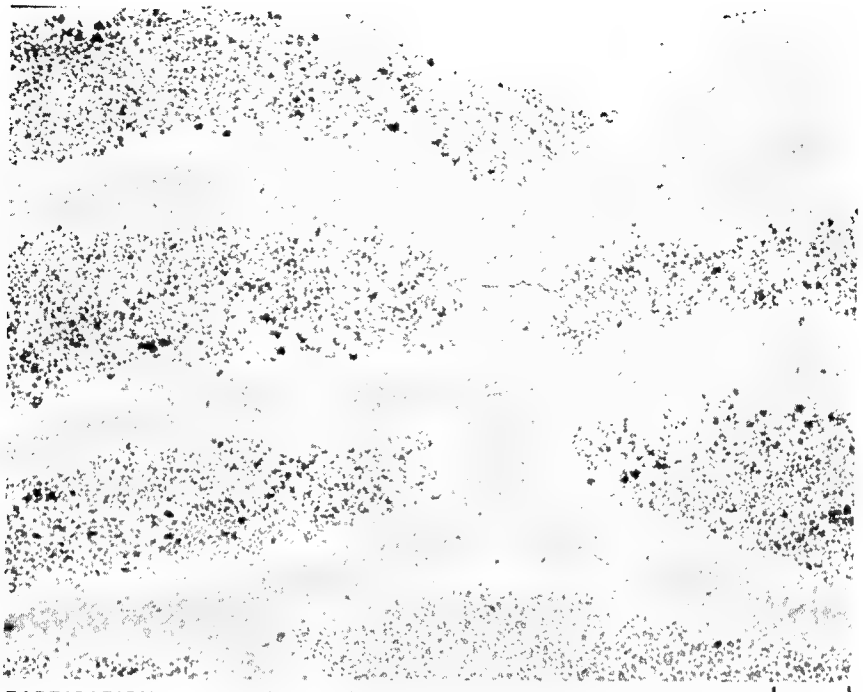

FABRICATION TRIAL 19 (6.9 MPa)

100μ

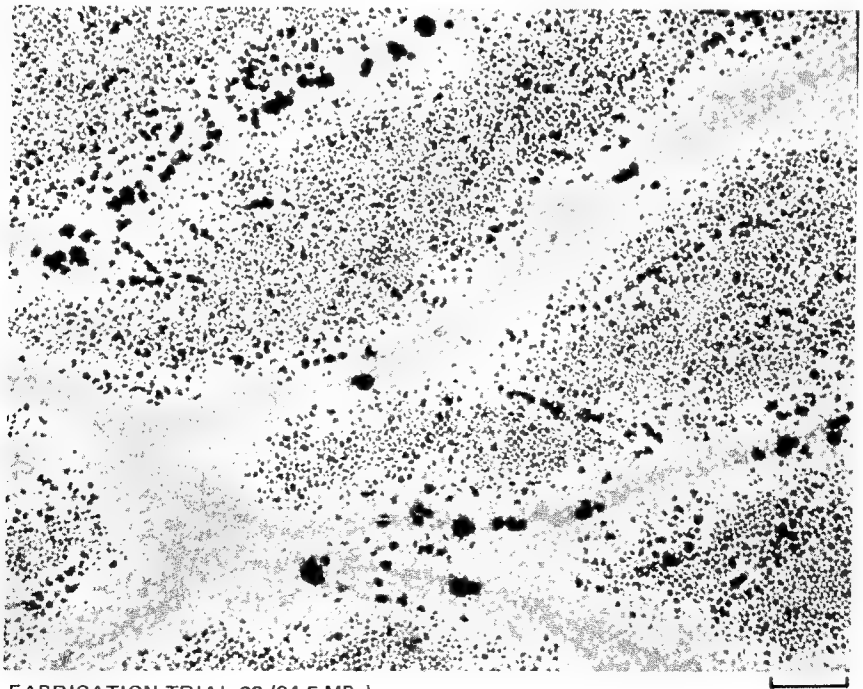

FABRICATION TRIAL 22 (34.5 MPa)

100μ

77–03–120–3

DRYWOUND AND PAINTED HMS/P–1700 POLYSULFONE

FABRICATION TRIAL 21

FABRICATION TRIAL 23

EFFECT OF IMPROVED TAPE DRYING ON HMS/P–1700 POLYSULFONE

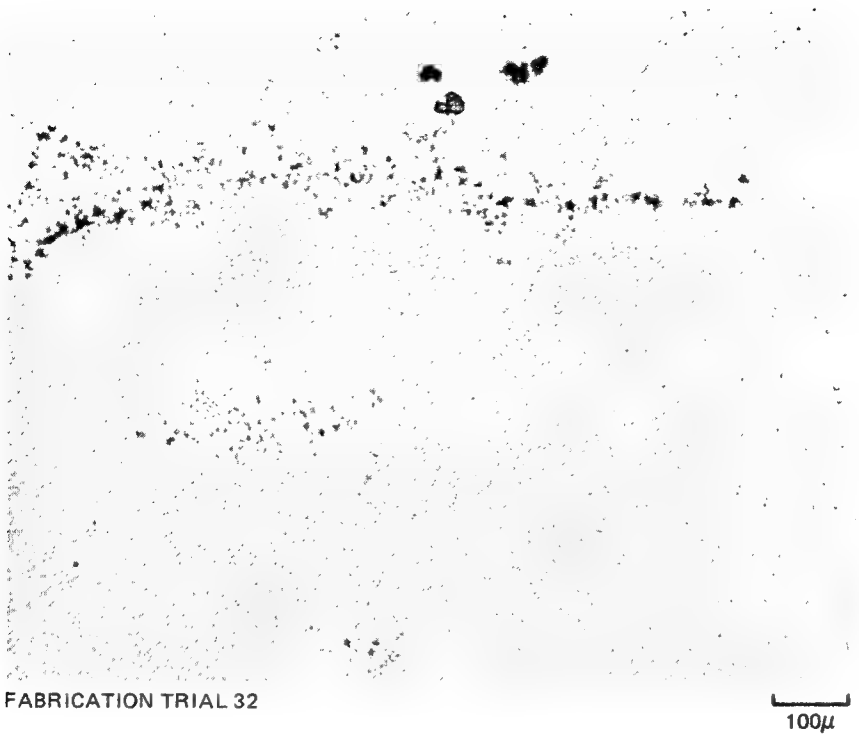

FABRICATION TRIAL 32

100μ

FABRICATION TRIAL 34

100μ

EFFECT OF TWO DRIVE SYSTEM ON HMS/P–1700 POLYSULFONE

77–03–120–2

EFFECT OF LONGER PRESSING TIMES ON HMS/P–1700 POLYSULFONE

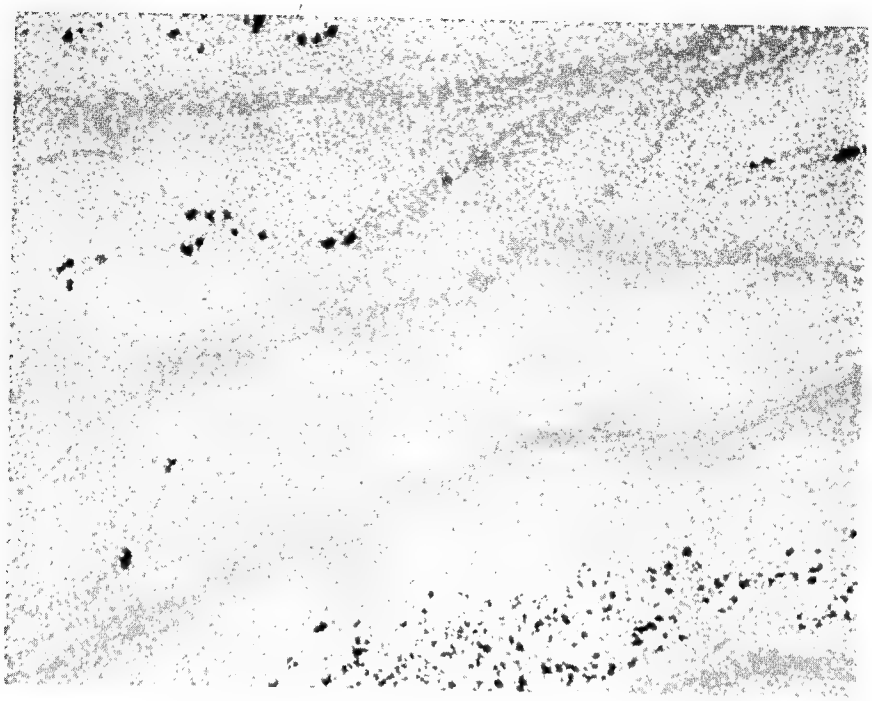

FABRICATION TRIAL 43(30 MIN.)

100 μ

FABRICATION TRIAL 44(60 MIN.)

100 μ

EFFECT OF VARIATION OF TEMPERATURE/PRESSURE ON HMS/300 P POLYETHERSULFONE

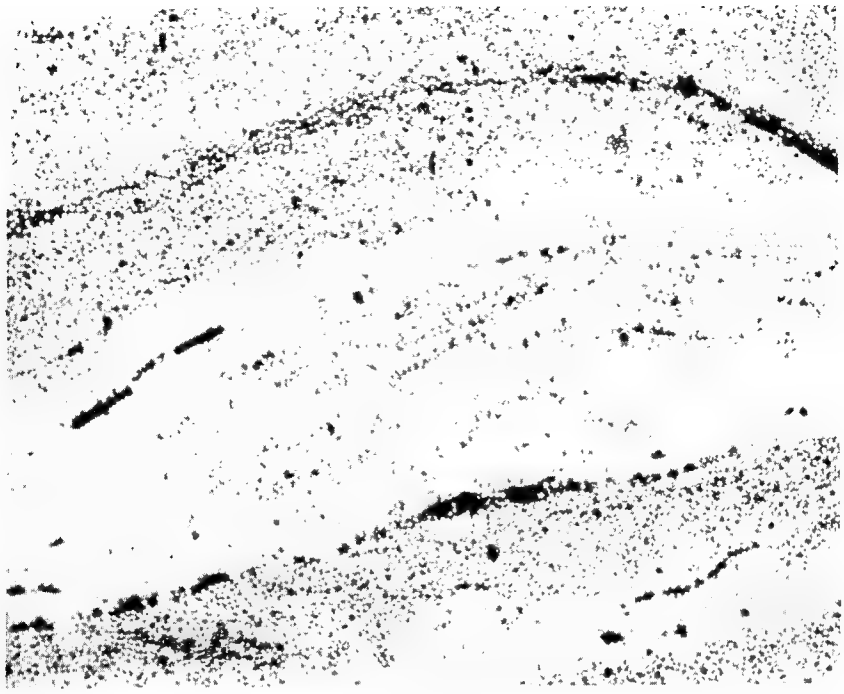

FABRICATION TRIAL 1 (315°C, 13.8 MPa)

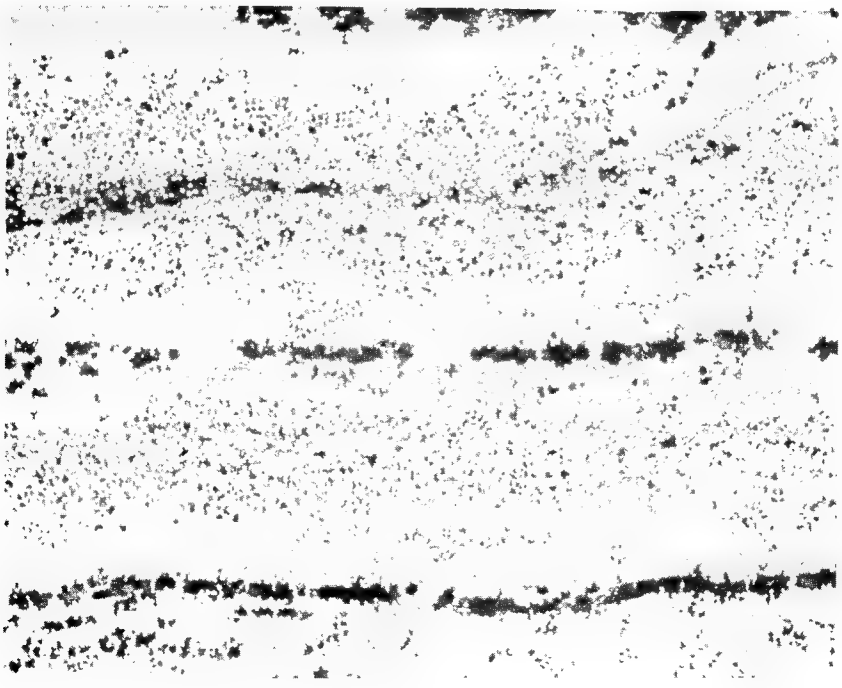

FABRICATION TRIAL 4 (370°C, 6.9 MPa)

77—03—143—4

HMS/300 P POLYETHERSULFONE WITH VOIDS BETWEEN BUNDLES

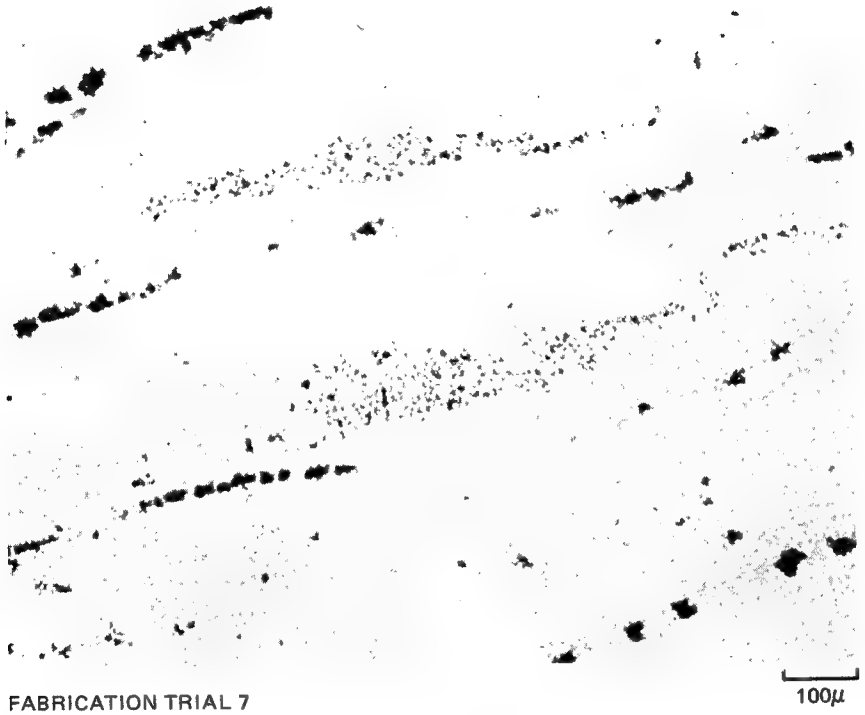

FABRICATION TRIAL 7

77–03–143–3

HMS/300 P POLYETHERSULFONE WITH 4 HRS. AT 150°C DRYING

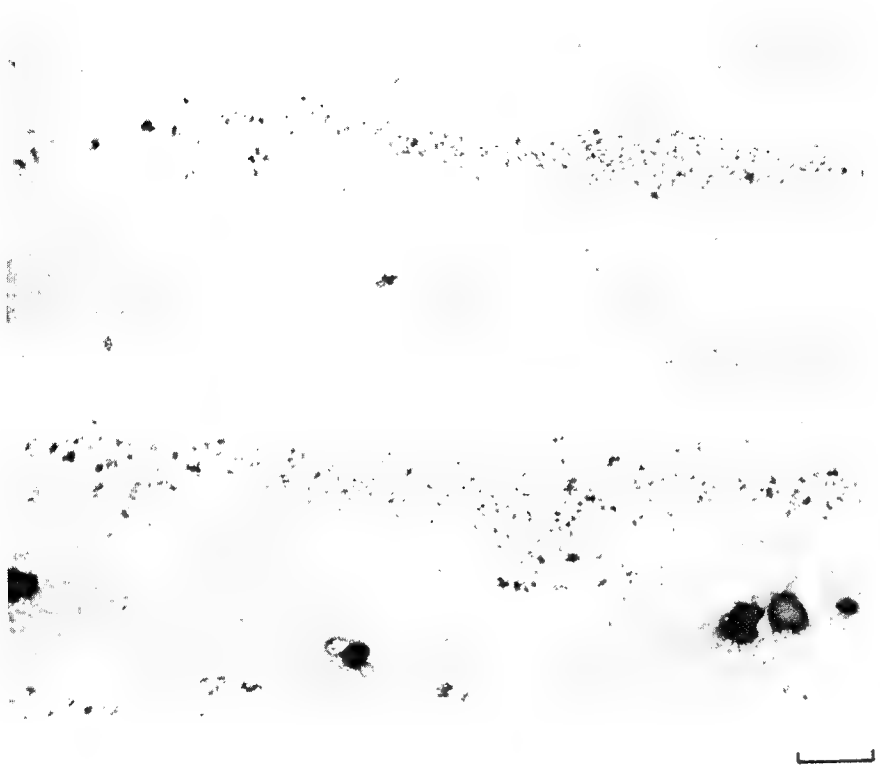

FABRICATION TRIAL 13

77-03-143-2

FIG. 11

OPTIMIZED HMS/300 P POLYETHERSULFONE COMPOSITE

FABRICATION TRIAL 20

100μ

77–03–143–1

FIG. 12

BASELINE FABRICATION PROCEDURE FOR HMS/360 POLYARYLSULFONE

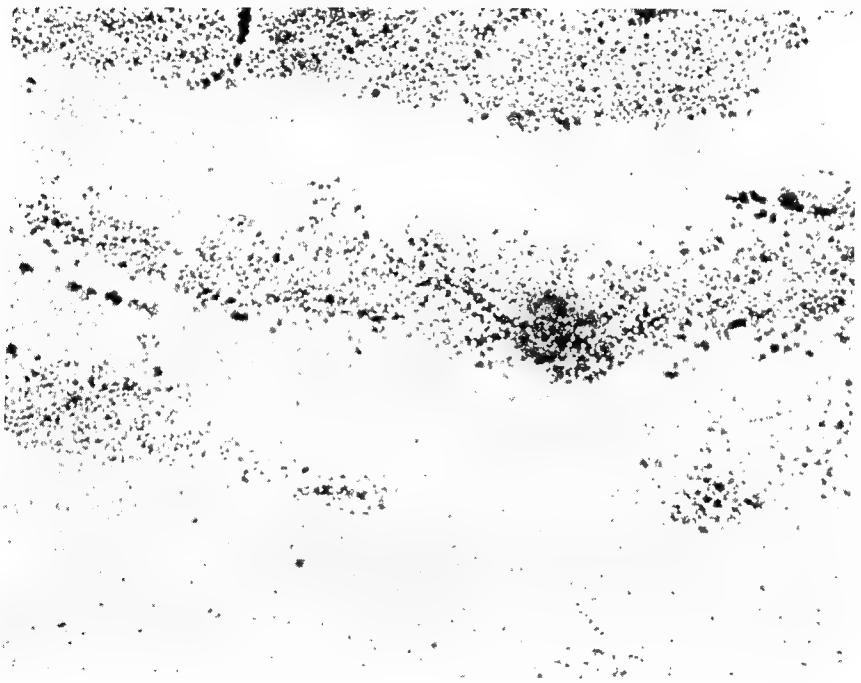

77-03-205-5

FIG. 13

HMS/360 POLYARYLSULFONE WITH 4 HRS. DRYING AT 150°C

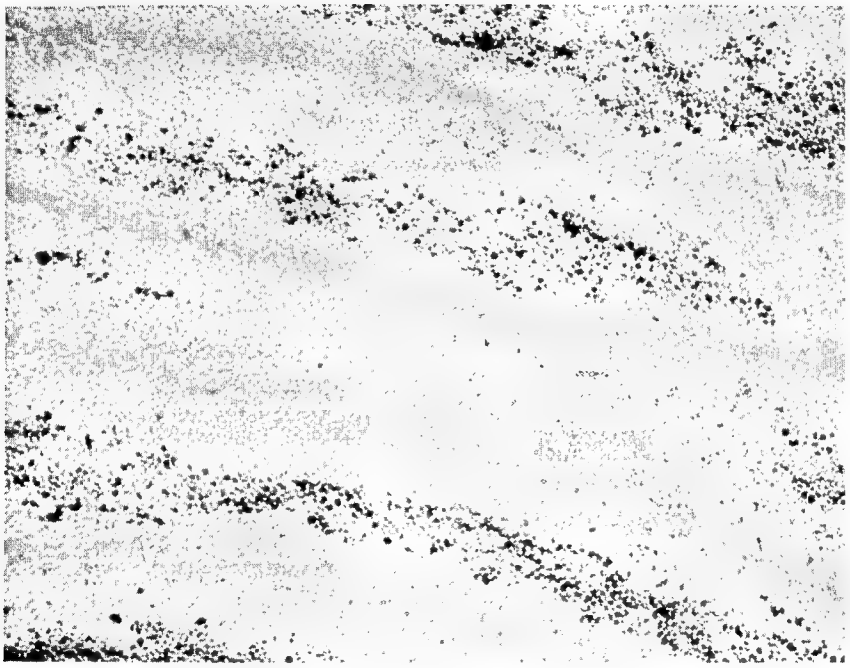

FABRICATION TRIAL 2

77-03-205-4

VARIATIONS IN CONSOLIDATION PRESSURE AND TEMPERATURE IN HMS/360 POLYARYLSULFONE

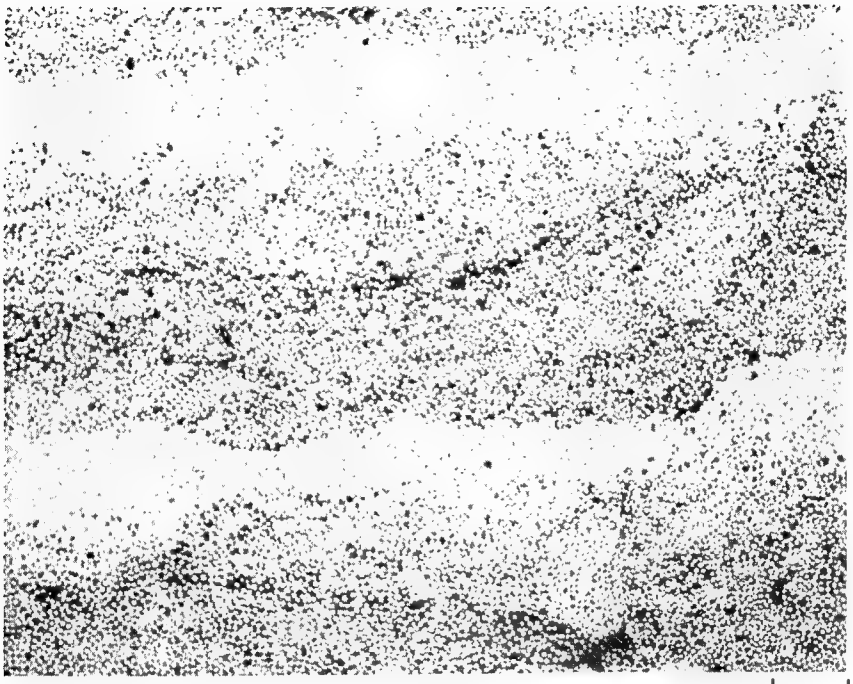

FABRICATION TRIAL 5 (343°C, 13.8 MPa)

100μ

FABRICATION TRIAL 6 (315°C, 13.8 MPa)

100μ

77-03-205-3

HMS/360 POLYARYLSULFONE CONSOLIDATED AT HIGH TEMPERATURE,HIGH PRESSURE

FABRICATION TRIAL 8

77—03—205—2

FIG. 16

OPTIMIZED HMS/360 POLYARYLSULFONE COMPOSITE

77-03-205-1

FIG. 17

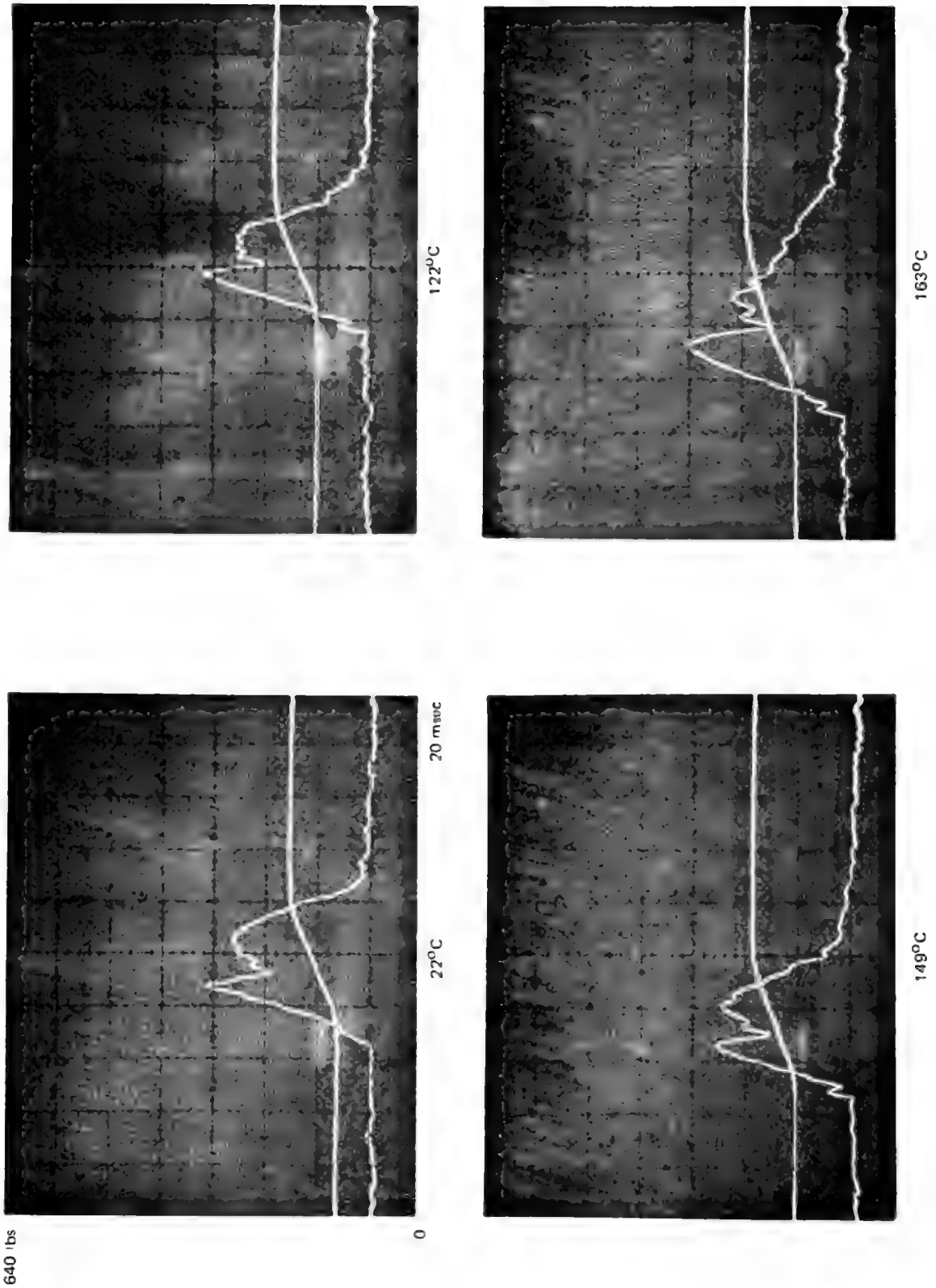

77-03-60-1

HMS/P–1700 POLYSULFONE STRESS–RUPTURE AT 122°C

± 45° ORIENTATION

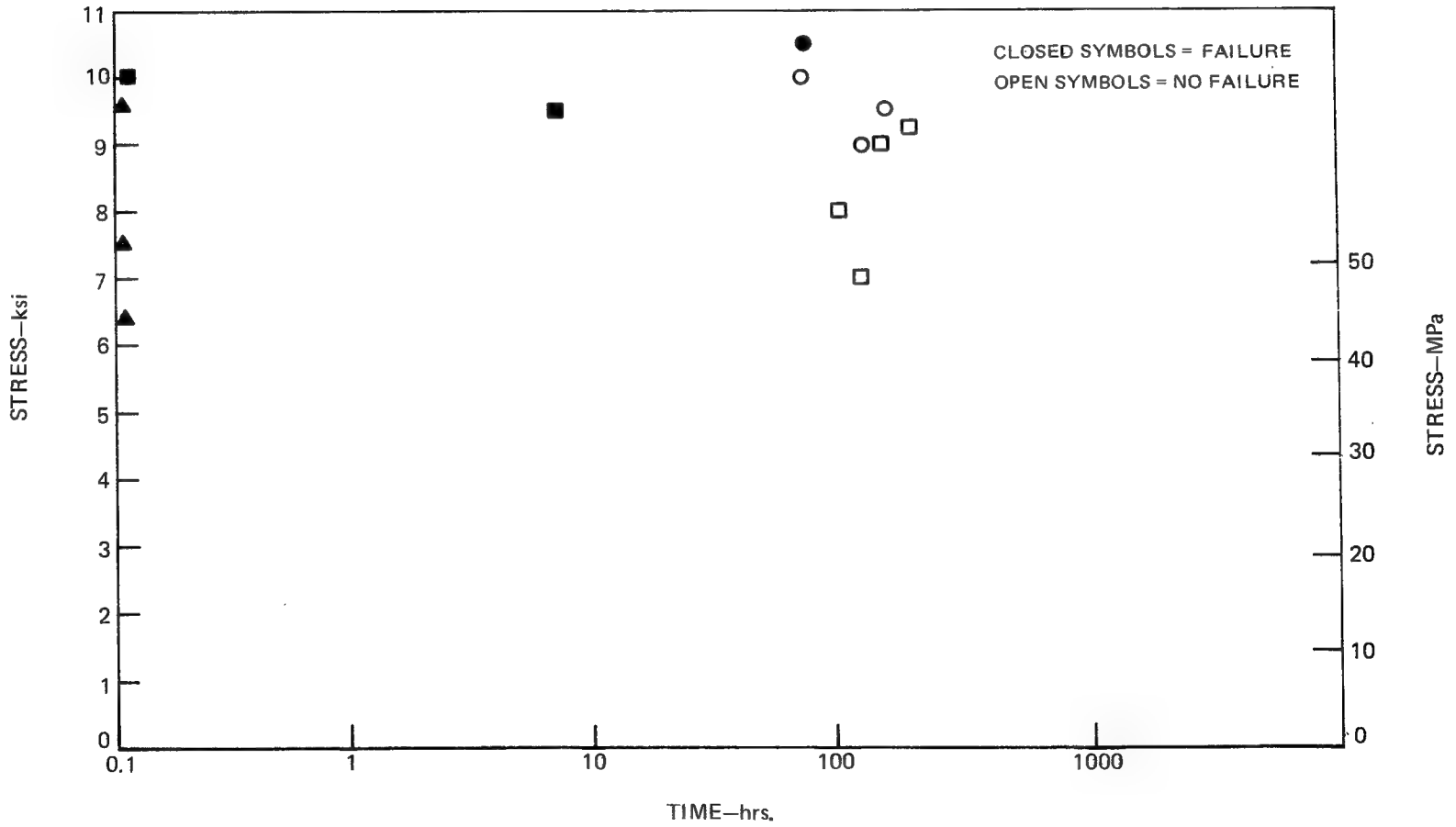

FIG. 18

77–03–79–3

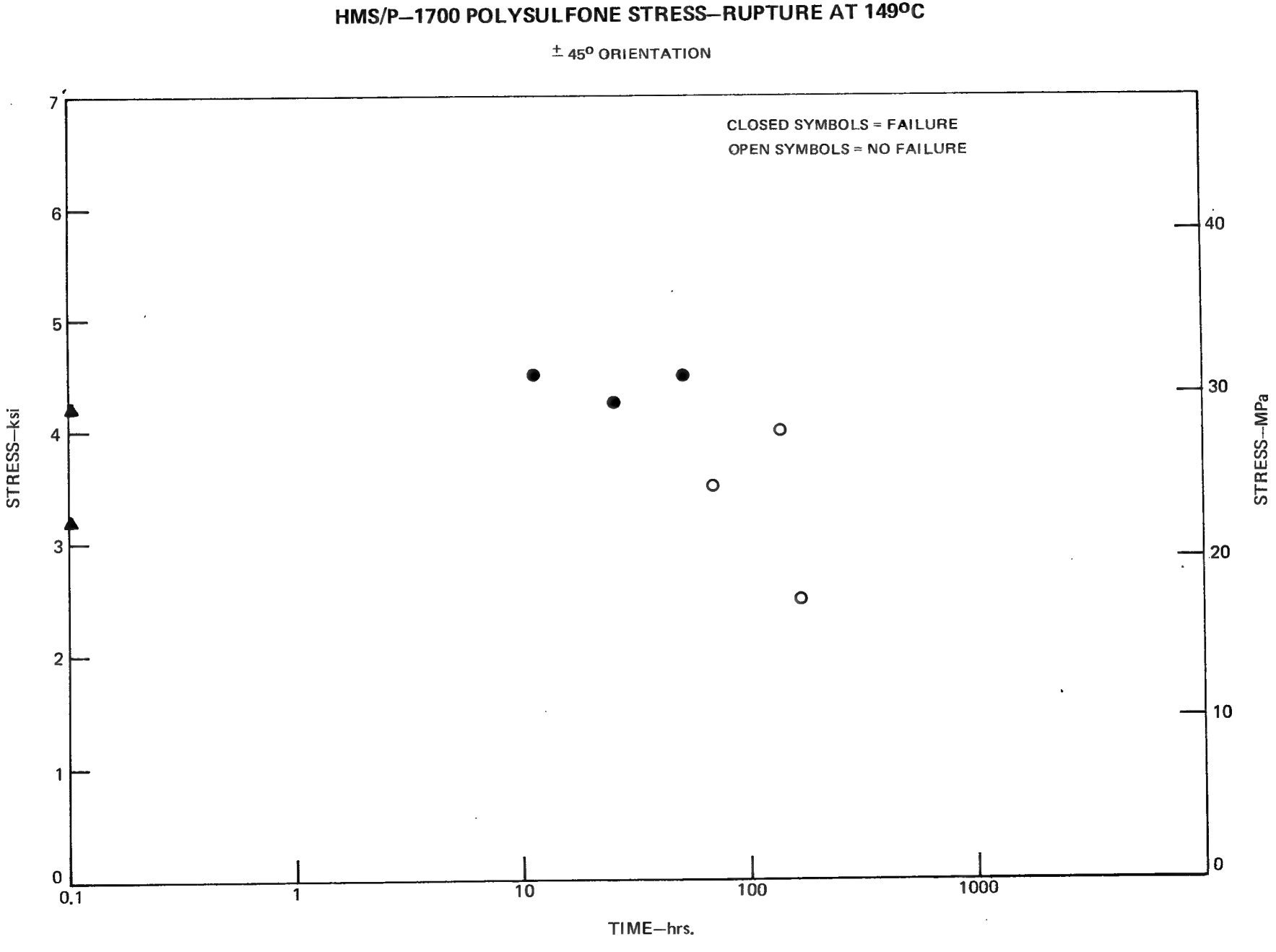

FIG. 19

77–03–79–2

FIG. 20

HMS/GLASS/P1700 POLYSULFONE THIN PENDULUM IMPACT TESTS

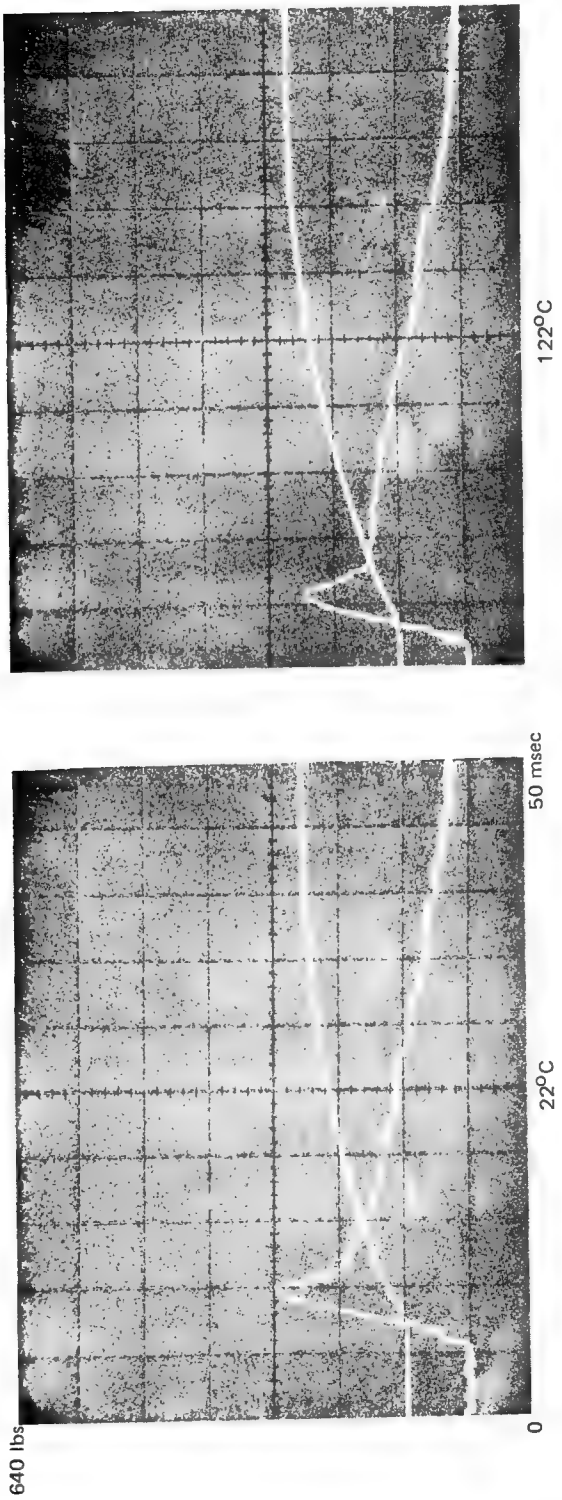

77-03-60-4

FIG. 21

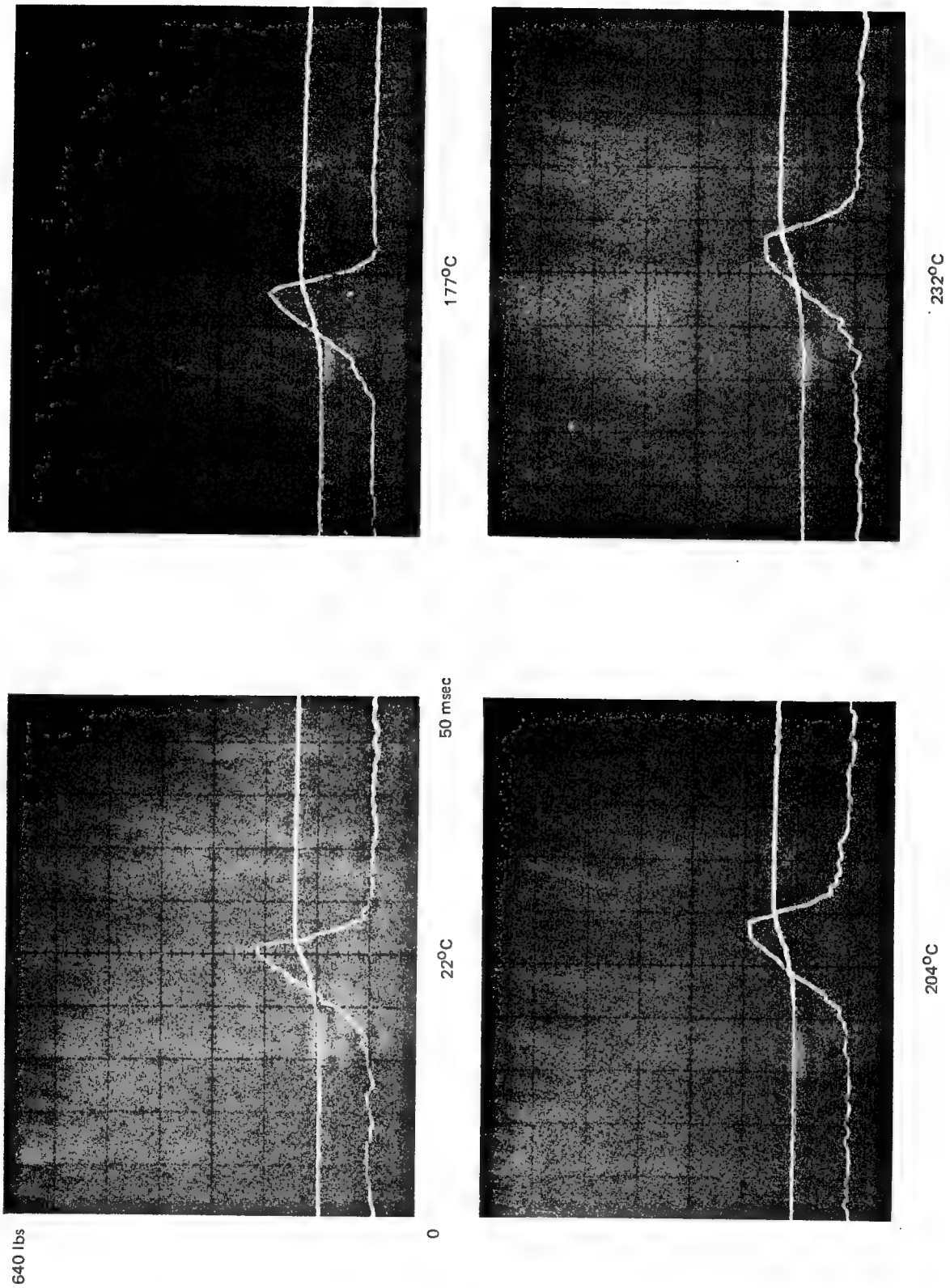

77-03-60-2

FIG. 23

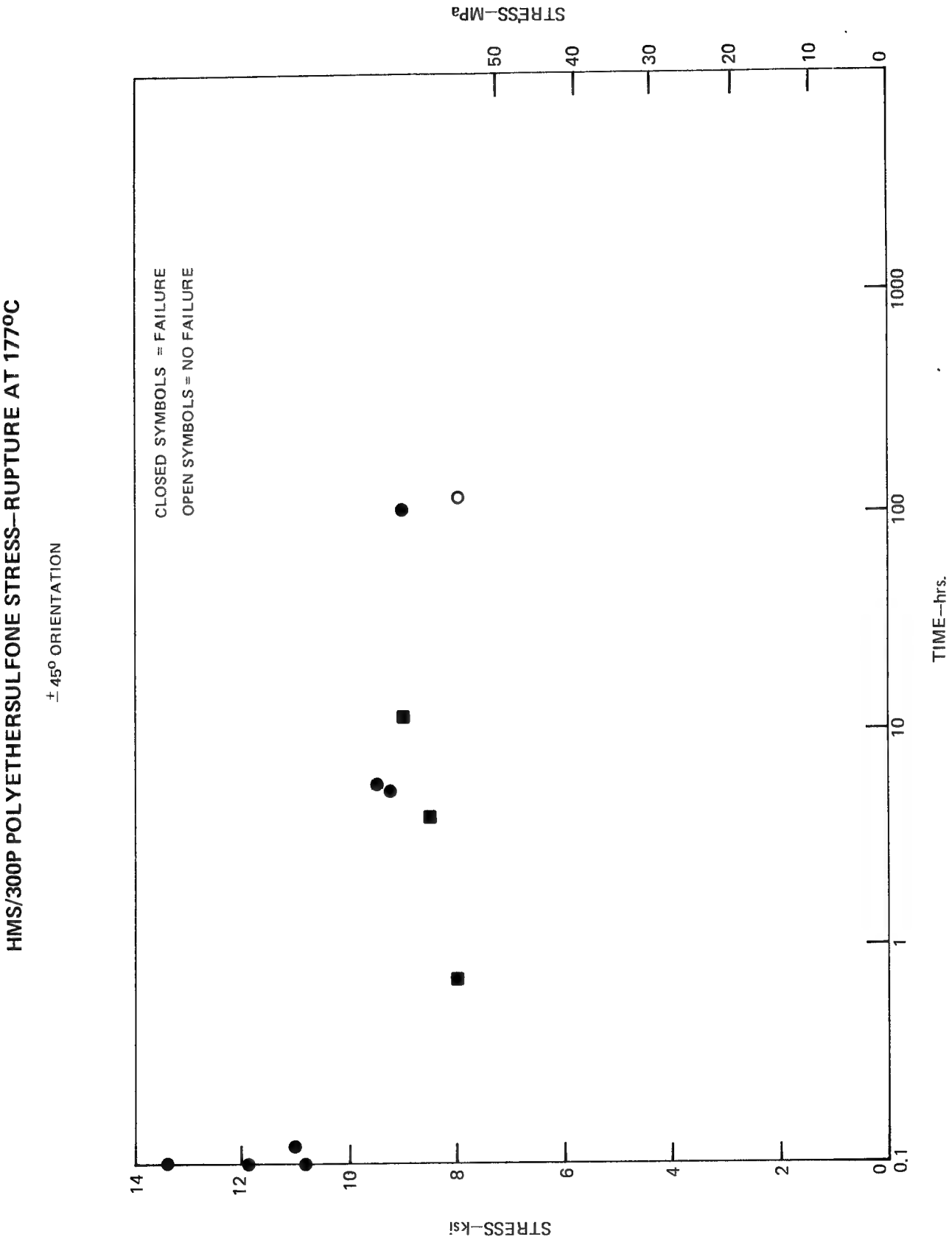

77–03–79–1

FIG. 22

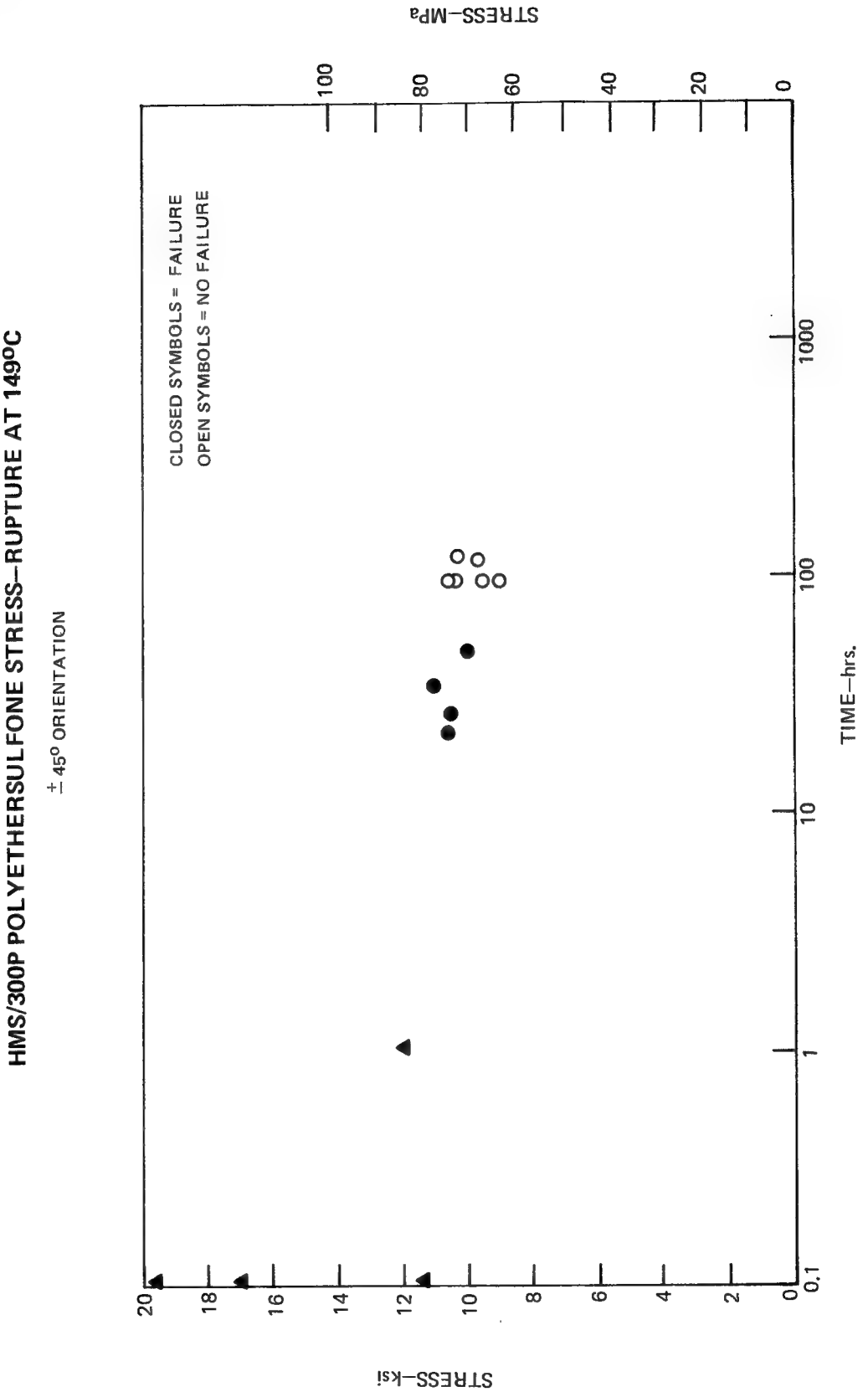

77–03–79–4

FIG. 24

HMS/ASTREL 360 POLYARYLSULFONE THIN PENDULUM IMPACT TESTS

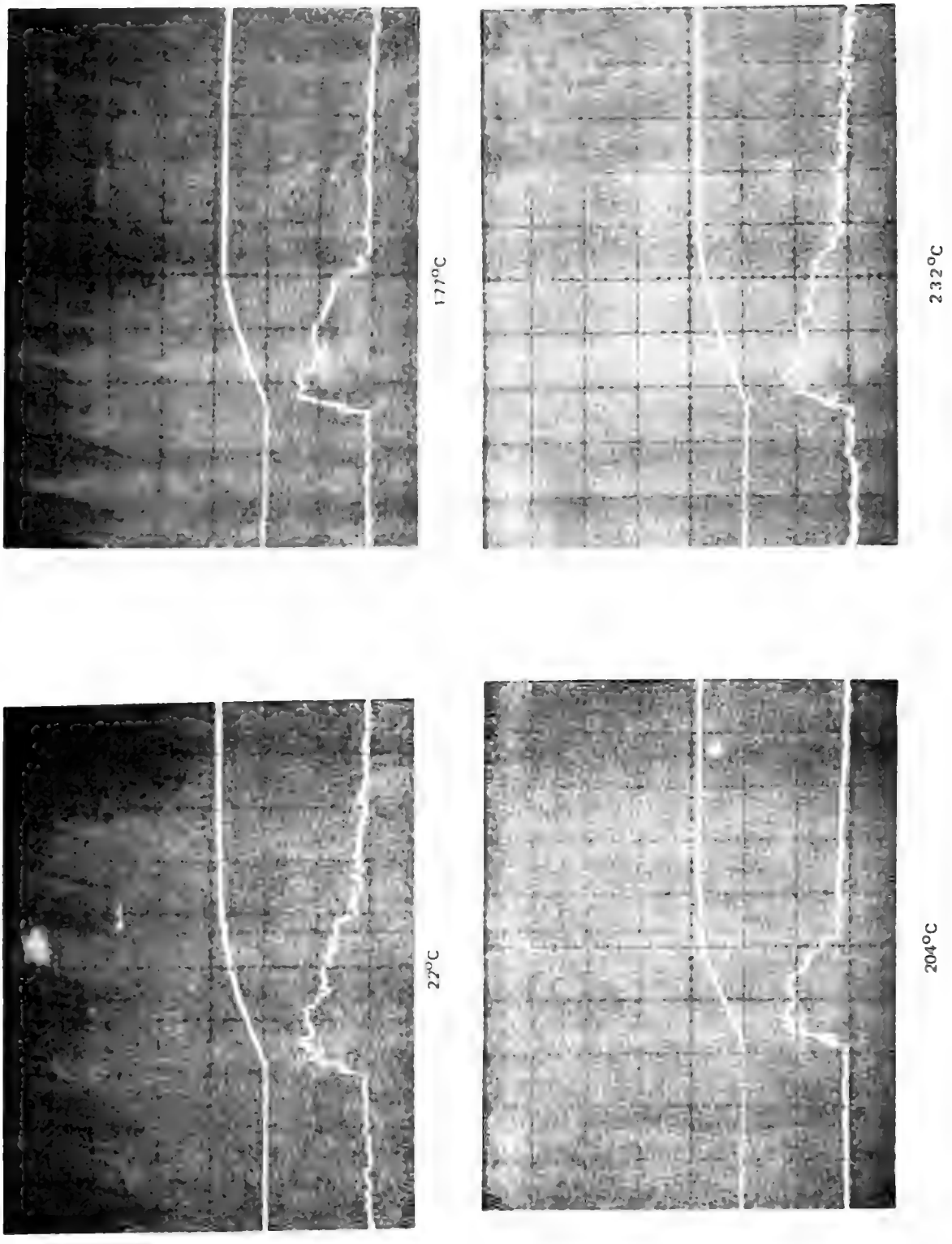

77-03-60-3

FIG. 25

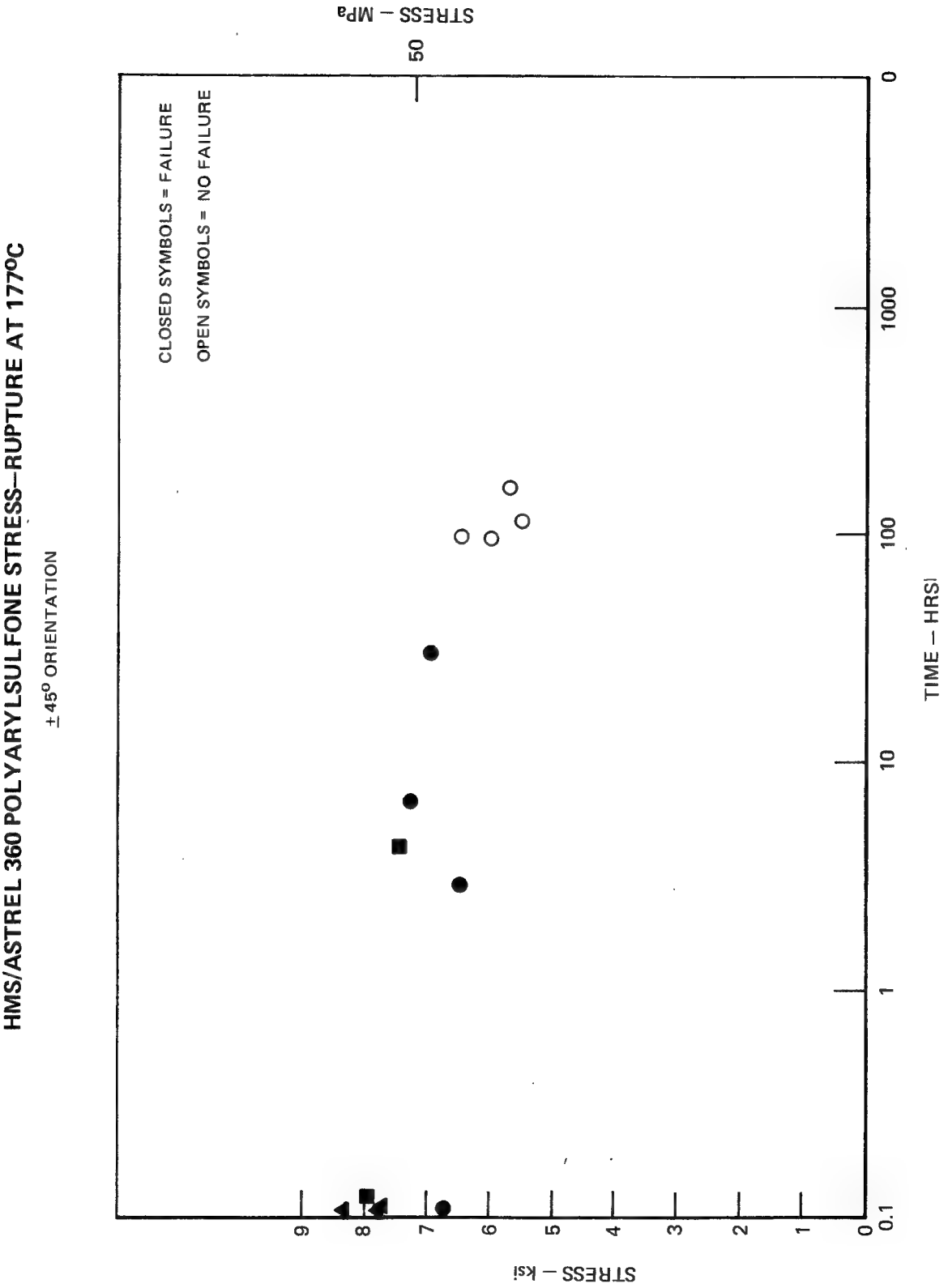

77–04–49–2

FIG. 26

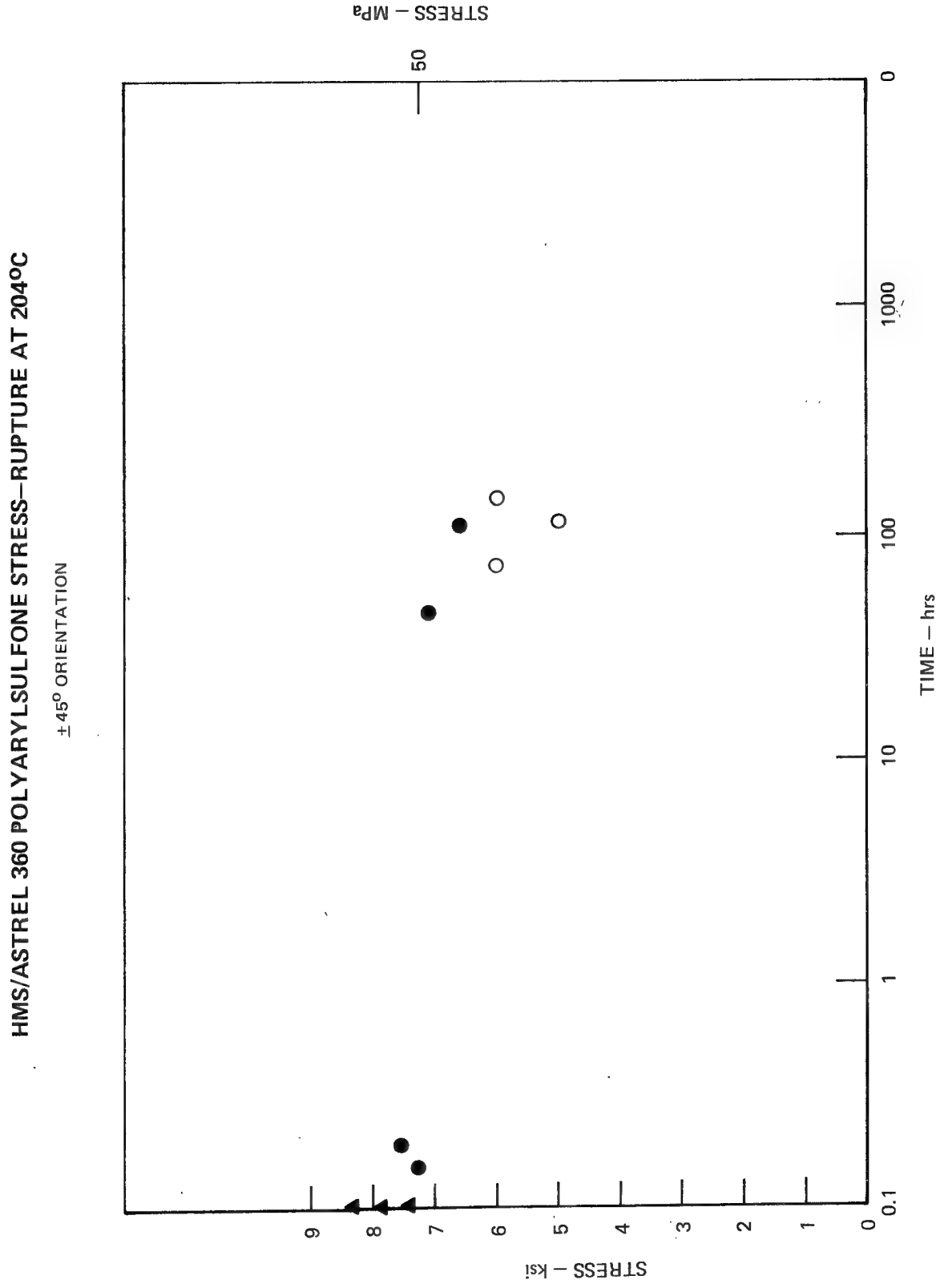

77–04–49–1

FIG. 27

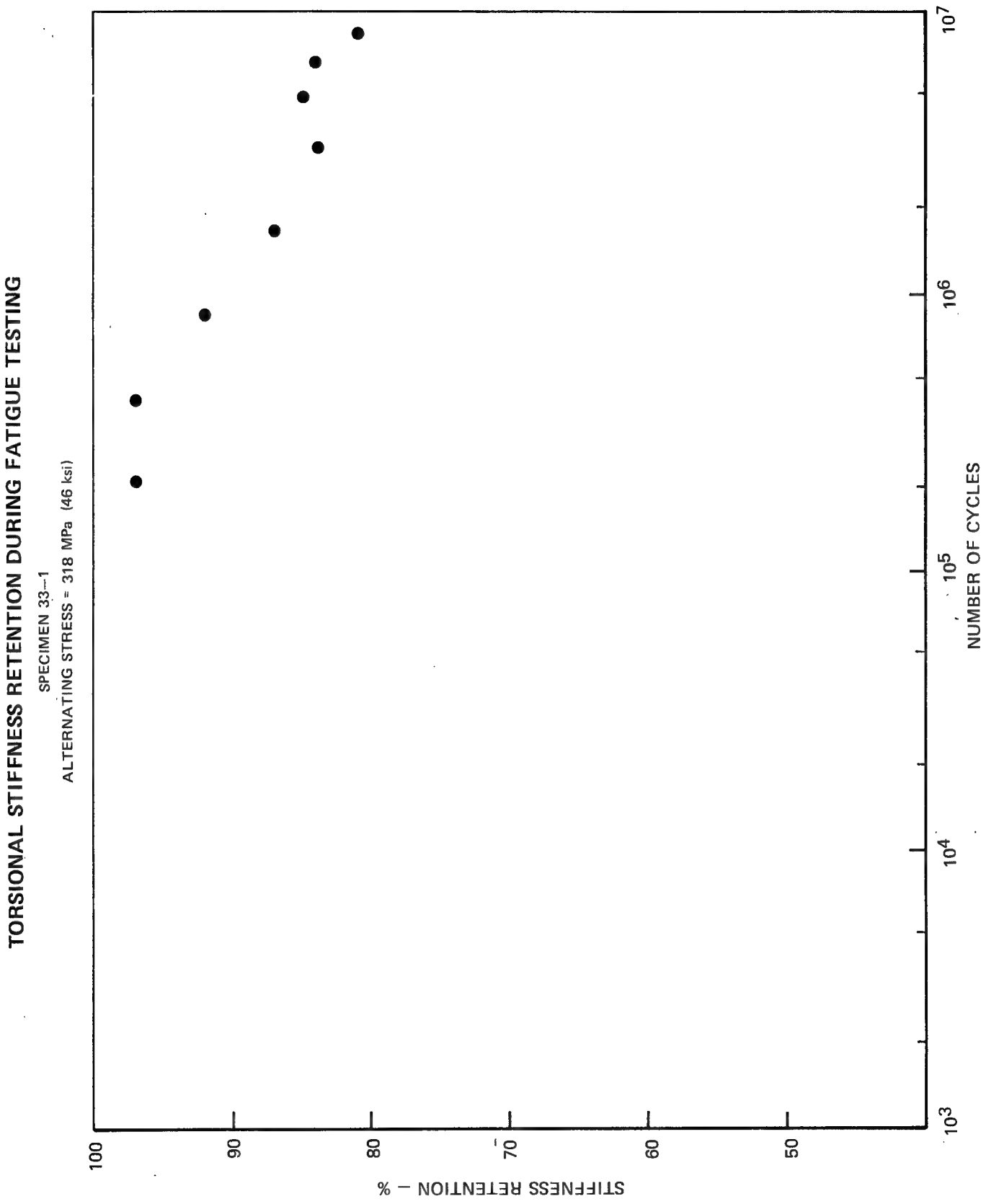

77–04–76–2

FIG. 28

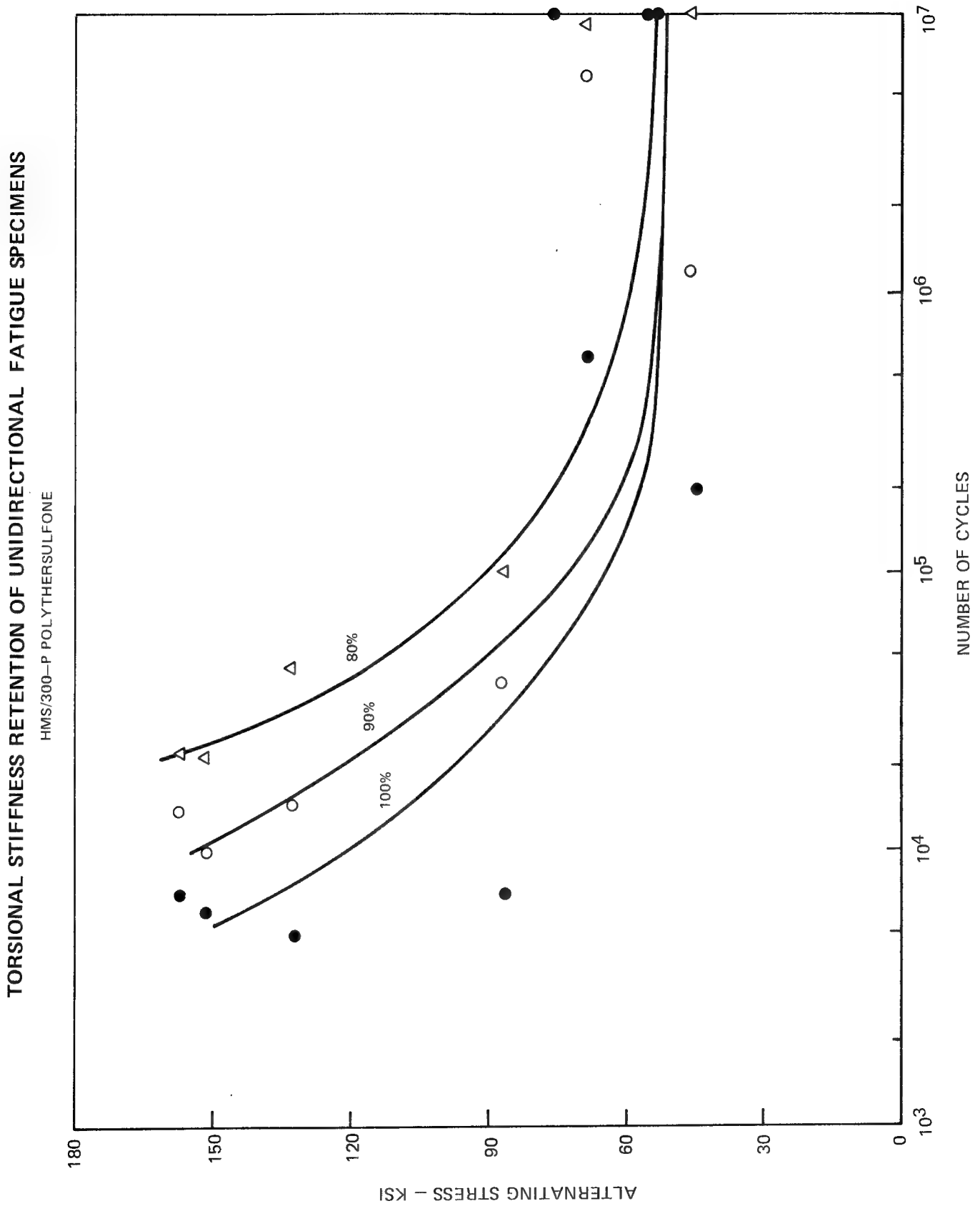

77-04-76-1

PLY ASSEMBLY

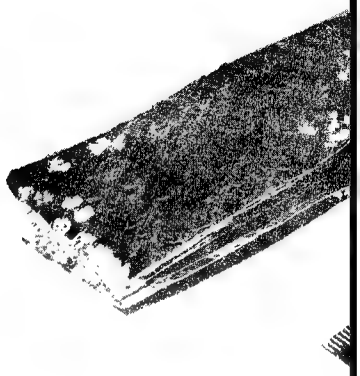

UN–DEBU

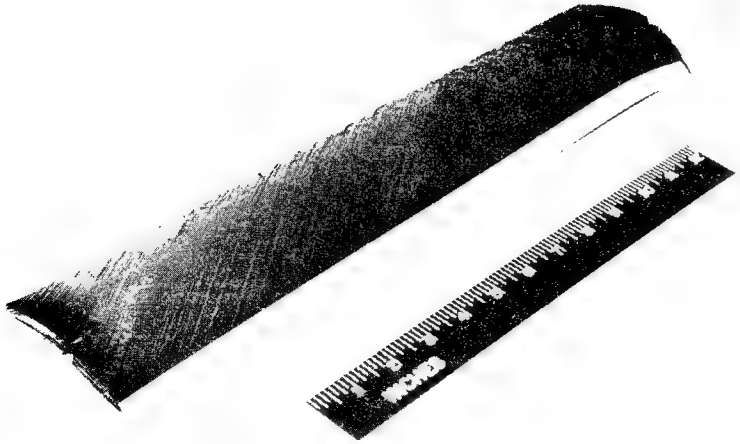

PREFORMED VANE

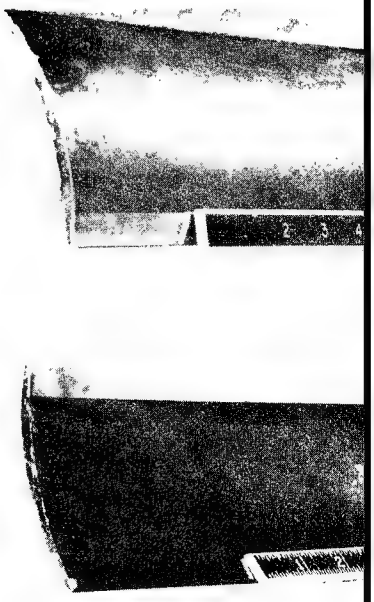

AS–

OPERATION SEQUENCE IN VANE FABRICATION

(2)

UN-DEBULKED LAYUP

LAYUP IN PREFOI

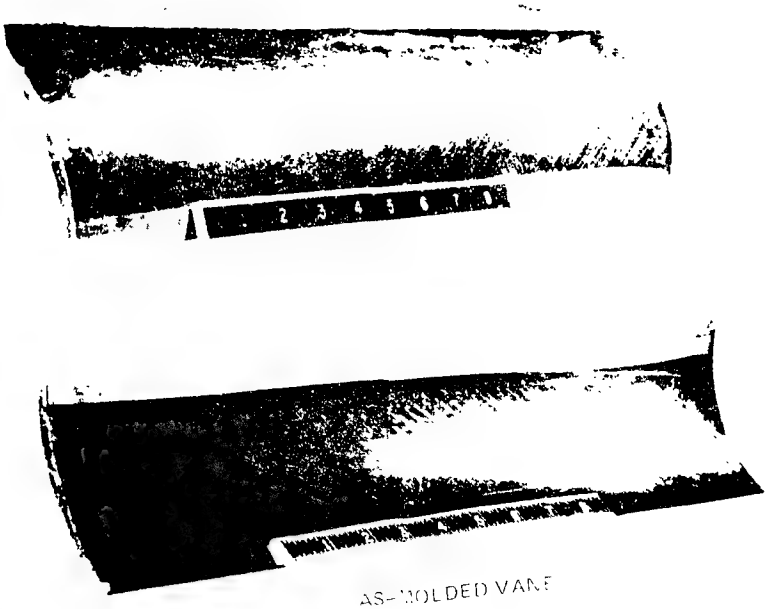

AS-MOLDED VANE

TRIMMED

CE IN VANE FABRICATION

2

KED LAYUP

3

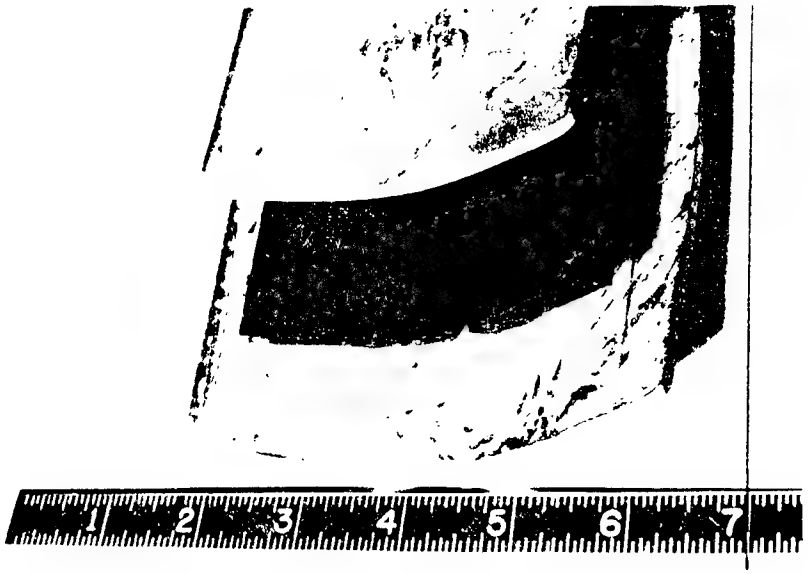

LAYUP IN PREFORM TOOL

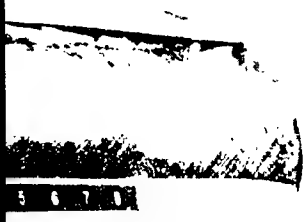

OLDED VANE

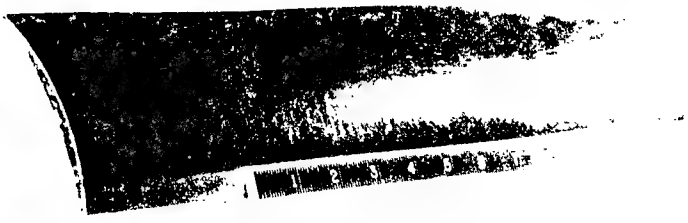

TRIMMED VANE

FIG. 30

COMPOSITE VANE WITH RUBBER FEET

77—04—49 -3

FIG. 31

FATIGUE TEST FIXTURE– THE FIXTURE SUPPORTS THE VANE AND APPLIES THE STATIC LOAD

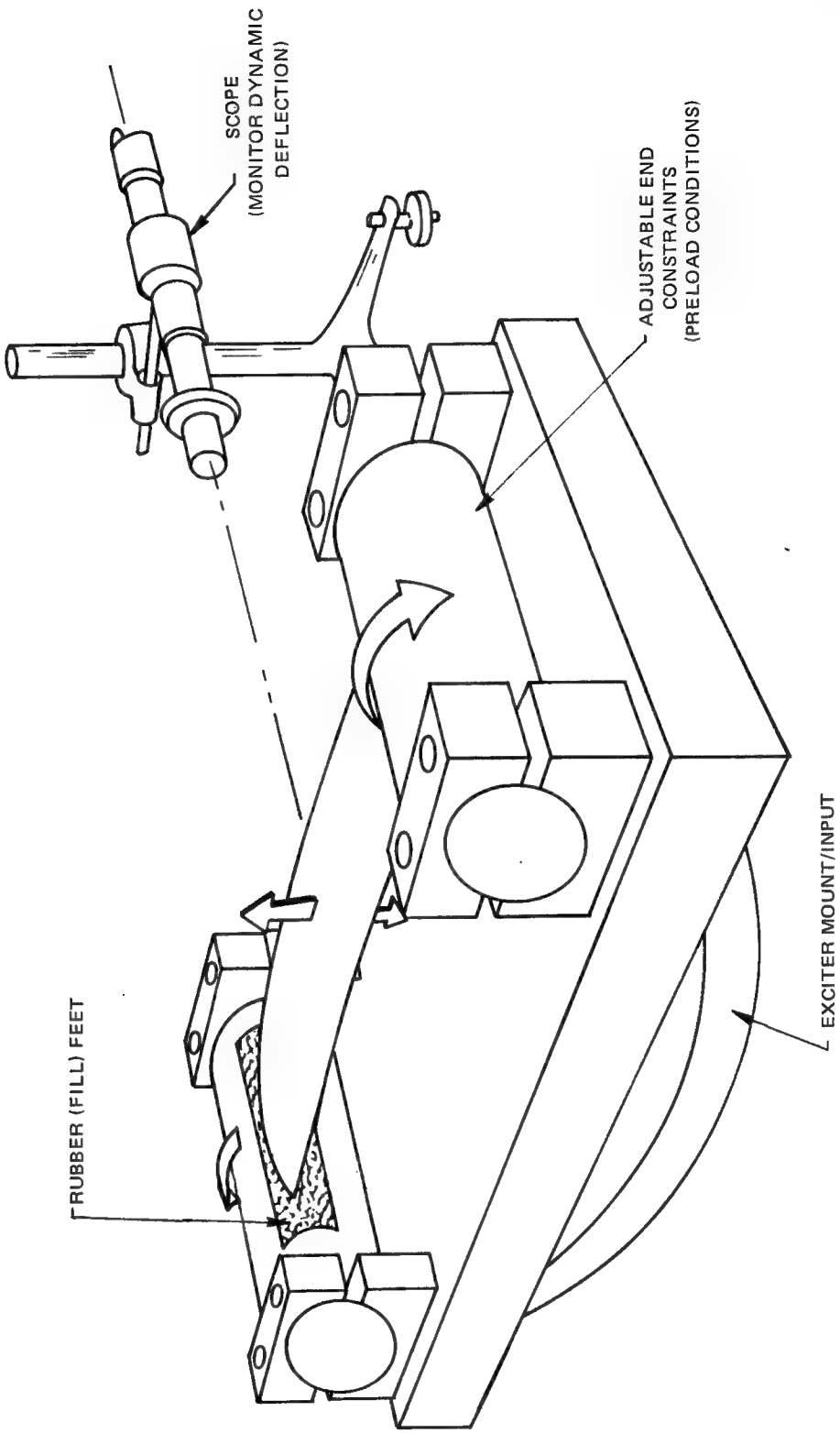

77–04–30–1

FIG. 32

FATIGUE FAILURE IN VANE TRAILING EDGE

77–04–110–1

DISTRIBUTION LIST

	Copies
National Aeronautics and Space Administration Lewis Research Center 21000 Brookpark Road Cleveland, Ohio 44135	
Attn: Contracting Officer, J. E. Hickey, MS 500-313	1
Technical Report Control Office, MS 5-5	1
Technology Utilization Office, MS 3-16	1
AFSC Liaison Office, MS 4-1	2
Library, MS 60-3	2
Office of Reliability & Quality Assurance, MS 500-111	1
R. H. Kemp, MS 49-1	1
K. J. Bowles, MS 49-1	25
N. T. Musial, MS 500-113	1
Annette Moran, MS 49-1	1
National Aeronautics and Space Administration Washington, D.C. 20546	
Attn: G. C. Deutsch/Code RW	1
J. J. Gangler/Code RWM	1
B. G. Achhammer/Code RWM	1
NASA Scientific and Technical Information Facility Attn: Acquisitions Branch P. O. Box 33 College Park, Maryland 20740	10
National Aeronautics and Space Administration Ames Research Center Moffett Field, California 94035	
Attn. Library	1
National Aeronautics and Space Administration Flight Research Center P. O. Box 273 Edwards, California 93523	
Attn: Library	1
National Aeronautics and Space Administration Goddard Space Flight Center Greenbelt, Maryland 20771	
Attn: Library	1

DISTRIBUTION LIST (continued)

	Copies
National Aeronautics and Space Administration John F. Kennedy Space Center Kennedy Space Center, Florida 32899	
Attn: Library	1
National Aeronautics and Space Administration Langley Research Center Langley Station Hampton, Virginia 23365	
Attn: V. L. Bell, MS 226	1
N. Johnston, MS 226	1
National Aeronautics and Space Administration Manned Spacecraft Center Houston, Texas 77001	
Attn: Library	1
Code EP	1
National Aeronautics and Space Administration George C. Marshall Space Flight Center Huntsville, Alabama 35812	
Attn: J. Curry	1
J. Stuckey	1
Jet Propulsion Laboratory 4800 Oak Grove Drive Pasadena, California 91103	
Attn: Library	1
Office of the Director of Defense Research and Engineering Washington, D.C. 20301	
Attn: Dr. H. W. Schulz, Office of Assistant Director (Chem. Technology)	1
Defense Documentation Center Cameron Station Alexandria, Virginia 22314	1

DISTRIBUTION LIST (continued)

	Copies
Research and Technology Division Bolling Air Force Base Washington, D.C. 20332	
Attn: RTNP	1
Bureau of Naval Weapons Department of the Navy Washington, D.C. 20360	
Attn: DLI-3	1
Director (Code 6180) U. S. Naval Research Laboratory Washington, D.C. 20390	
Attn: H. W. Carhart	1
Picatinny Arsenal Dover, New Jersey	
Attn: SMUPA-VP3	1
Structural Composites Industries, Inc. 6344 North Irwindale Avenue Azusa, California 91703	
Attn: Ira Petker	1
Aeronautic Division of Philco Corporation Ford Road Newport Beach, California 92600	
Attn: Dr. L. H. Linder, Manager Technical Information Department	1
Aerospace Corporation P. O. Box 95085 Los Angeles, California 90045	
Attn: Library Documents	1
Aerotherm Corporation 800 Welch Road Palo Alto, California 94304	
Attn: Mr. R. Rindal	1

DISTRIBUTION LIST (continued)

	Copies
General Dynamics Convair Aerospace Division P.O. Box 748 Fort Worth, Texas 76101	
Attn: Tech. Library, 6212	1
Material Science Corporation 1777 Walton Road Blue Bell, Pennsylvania 19422	
Attn: Ms. N. Sabia	1
Fiber Science Inc. 245 East 157 Street Gardena, California 90248	
Attn: L. J. Ashton	1
U.S. Army Air Mobility R&D Lab Fort Eustis, Virginia 23604	
Attn: Mr. H. L. Morrow, SAVDL-EU-TAP	1
U.S. Army Aviation Systems Command P.O. Box 209, Main Office St. Louis, Missouri 63166	
Attn: Mr. Ronald Evers	1
United States Air Force Aero Propulsion Laboratory Wright-Patterson AFB, Ohio 45433	
Attn: Mr. T. J. Norbut, AFAPL/TBP	1
Air Force Materials Laboratory Wright-Patterson AFB, Ohio 45433	
Attn: Mr. Paul Pirrung, AFML/LTN	1
Allison Division of Detroit Diesel Company P.O. Box 894 Department 5827, S42 Indianapolis, Indiana 46206	
Attn: John Spees	1

DISTRIBUTION LIST (continued)

	Copies
Air Force Materials Laboratory Wright-Patterson Air Force Base, Ohio 45433	
Attn: AFML/MBC, T. J. Reinhart, Jr.	1
AFML/LNC, D. L. Schmidt	1
Office of Aerospace Research (RROSP) 1400 Wilson Boulevard Arlington, Virginia 22209	
Attn: Major Thomas Tomaskovic	1
Arnold Engineering Development Center Air Force Systems Command Tullahoma, Tennessee 37389	
Attn: AEOIM	1
Air Force Systems Command Andrews Air Force Base Washington, D.C. 20332	
Attn: SCLT/Capt. S. W. Bowen	1
Air Force Rocket Propulsion Laboratory Edwards, California 93523	
Attn: RPM	1
Air Force Flight Test Center Edwards Air Force Base, California 93523	
Attn: FTAT-2	1
Air Force Office of Scientific Research Washington, D.C. 20333	
Attn: SREP, Dr. J. F. Masi	1
American Cyanamid Company 1937 West Main Street Stamford, Connecticut 06902	
Attn: Security Officer	1
AVCO Corporation Space Systems Division Lowell Industrial Park Lowell, Massachusetts 01851	
Attn: W. Port	1

DISTRIBUTION LIST (continued)

	Copies
Battelle Memorial Institute 505 King Avenue Columbus, Ohio 43201	
Attn: Report Library, Room 6A	1
Bell Aerosystems, Inc. Box 1 Buffalo, New York 14205	
Attn: T. Reinhardt	1
The Boeing Company Aero Space Division P. O. Box 3999 Seattle, Washington 98124	
Attn: J. T. Hoggatt	1
Celanese Research Company Morris Court Summit, New Jersey	
Attn: Dr. J. R. Leal	1
University of Denver Denver Research Institute P. O. Box 10127 Denver, Colorado 80210	
Attn: Security Office	1
Dow Chemical Company Security Section Box 31 Midland, Michigan 48641	
Attn: Dr. R. S. Karpiuk, 1710 Building	1
E. I. DuPont De Nemours & Co. (Inc.) Fibers Department Experimental Station - Bldg. 262 Wilmington, Delaware 19898	
Attn: Dr. Carl Zweben	1

DISTRIBUTION LIST (continued)

	Copies
Ultrasystems, Inc. 2400 Michelson Drive Irvine, California 92664	
Attn: Dr. R. Kratzer	1
General Dynamics/Convair Dept. 643-10 Kerny Mesa Plant San Diego, California 92112	
Attn: J. Hertz	1
General Electric Company Re-Entry Systems Department P. O. Box 8555 Philadelphia, Pennsylvania 19101	
Attn: Library	1
General Electric Company Technical Information Center N-32, Building 700 Cincinnati, Ohio	
Attn: C. A. Steinhagen	1
C. L. Stotler	1
General Technologies Corporation 708 North West Street Alexandria, Virginia	
Attn: W. M. Powers	1
Grumman Aerospace Corporation Plant 12, Dept. 447 Bethpage, New York	
Attn: N. A. Sullo	1
Hercules Powder Company Allegheny Ballistics Laboratory P. O. Box 210 Cumberland, Maryland 21501	
Attn: Library	1

DISTRIBUTION LIST (continued)

	Copies
Union Carbide Corporation 12900 Snow Road Parma, Ohio	
Attn: Library	1
United Aircraft Corporation United Aircraft Research Laboratories East Hartford, Connecticut 06118	
Attn: D. A. Scola	1
United Aircraft Corporation Pratt and Whitney Aircraft East Hartford, Connecticut 06108	
Attn: G. Wood	1
United Aircraft Corporation United Technology Center P. O. Box 358 Sunnyvale, California 94088	
Attn: Library	1
Westinghouse Electric Corporation Westinghouse Research Laboratories Pittsburgh, Pennsylvania	
Attn: Library	1
Whittaker Corporation Research & Development/San Diego 3540 Aero Court San Diego, California 92123	
Attn: R. Gosnell	1
TRW Systems One Space Park Redondo Beach, California 90278	
Attn: Dr. E. A. Burns, Bldg. 01, Room 2020	3

DISTRIBUTION LIST (continued)

	Copies
Hughes Aircraft Company Culver City, California	
Attn: N. Bilow	1
ITT Research Institute Technology Center Chicago, Illinois 60616	
Attn: C. K. Hersh, Chemistry Division	1
Lockheed Missiles & Space Company Propulsion Engineering Division (D.55-11) 111 Lockheed Way Sunnyvale, California 94087	1
McDonnell Douglas Aircraft Company Santa Monica Division 3000 Ocean Park Blvd. Santa Monica, California 90406	
Attn: N. Byrd	1
Monsanto Research Corporation Dayton Laboratory Station B, Box 8 Dayton, Ohio 45407	
Attn: Library	1
North American Rockwell Corporation Space & Information Systems Division 12214 Lakewood Blvd. Downey, California 90242	
Attn: Technical Information Center D/096-722 (AJ01)	1
Northrop Corporate Laboratories Hawthorne, California 90250	
Attn: Library	1
Rocketdyne, A Division of North American Rockwell Corporation 6633 Canoga Avenue Canoga Park, California 91304	
Attn: Library, Dept. 596-306	1